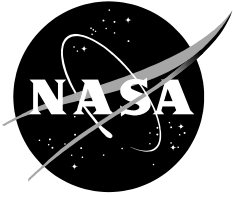


NASA/TM–20230003164



# Experimental Aeroheating Study in NASA LaRC 20-Inch Mach 6 Air Tunnel: Discrete Roughness on BOLT – Test 7071

*Scott A. Berry and Carey F. Scott, Jr.  
Langley Research Center, Hampton, Virginia*

---

**April 2023**

## NASA STI Program Report Series

The NASA STI Program collects, organizes, provides for archiving, and disseminates NASA's STI. The NASA STI program provides access to the NTRS Registered and its public interface, the NASA Technical Reports Server, thus providing one of the largest collections of aeronautical and space science STI in the world. Results are published in both non-NASA channels and by NASA in the NASA STI Report Series, which includes the following report types:

- **TECHNICAL PUBLICATION.** Reports of completed research or a major significant phase of research that present the results of NASA Programs and include extensive data or theoretical analysis. Includes compilations of significant scientific and technical data and information deemed to be of continuing reference value. NASA counterpart of peer-reviewed formal professional papers but has less stringent limitations on manuscript length and extent of graphic presentations.
- **TECHNICAL MEMORANDUM.** Scientific and technical findings that are preliminary or of specialized interest, e.g., quick release reports, working papers, and bibliographies that contain minimal annotation. Does not contain extensive analysis.
- **CONTRACTOR REPORT.** Scientific and technical findings by NASA-sponsored contractors and grantees.
- **CONFERENCE PUBLICATION.** Collected papers from scientific and technical conferences, symposia, seminars, or other meetings sponsored or co-sponsored by NASA.
- **SPECIAL PUBLICATION.** Scientific, technical, or historical information from NASA programs, projects, and missions, often concerned with subjects having substantial public interest.
- **TECHNICAL TRANSLATION.** English-language translations of foreign scientific and technical material pertinent to NASA's mission.

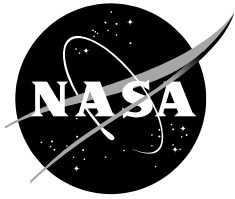
Specialized services also include organizing and publishing research results, distributing specialized research announcements and feeds, providing information desk and personal search support, and enabling data exchange services.

For more information about the NASA STI program, see the following:

- Access the NASA STI program home page at <http://www.sti.nasa.gov>
- Help desk contact information:

<https://www.sti.nasa.gov/sti-contact-form/> and select the "General" help request type.

NASA/TM–20230003164



# Experimental Aeroheating Study in NASA LaRC 20-Inch Mach 6 Air Tunnel: Discrete Roughness on BOLT – Test 7071

*Scott A. Berry and Carey F. Scott, Jr.  
Langley Research Center, Hampton, Virginia*

National Aeronautics and  
Space Administration

*Langley Research Center  
Hampton, Virginia 23681-2199*

---

**April 2023**

## **Acknowledgments**

The authors would like to acknowledge a number of folks who supported this study behind the scenes. The model was designed by NASA LaRC and built under contract at Calspan in Newport News, VA. The model design was completed by Sean McCormick, with support from Kevin Bonilla, Ray Rhew, Mark Cagle, Mike Langford, Doug Weber, and Sheryl Kopczynski. Model fabrication was completed with assistance from Chris Angel, Brett Jones, Neil Lewis, Lawrence Layman, Lawrence Stippich, Mylika Wade, Will Nowell, Brandon Goding, Chamell Ashley, Antoine Snipes, Daniel Diaz, David Martel, David Martin, David Sallee, Markus McMurray, Rich Phebus, Richard Smith, Samuel Fatony, John Tyminski, Jock Mckellar, Richard Schmidt, Thomas Grafton, Justin Gann, Lytonia Spigner, Matthew Reno, Barry Twine, David Golub, Jason Alholinna, and Steven Simmons. Model quality assurance and application of surface fiducial marks was completed by Clint Reese. Tunnel test operations were provided by Johnny Ellis, Kevin Hollingsworth and Nick Shaw, with air handling support from Robert Edwards, Michael Fuscia, and Dave Gary.

<p>The use of trademarks or names of manufacturers in this report is for accurate reporting and does not constitute an official endorsement, either expressed or implied, of such products or manufacturers by the National Aeronautics and Space Administration</p>
--

This report is available in electronic form at  
<http://ntrs.nasa.gov>

THIS PAGE INTENTIONALLY LEFT BLANK

## **Abstract**

An experimental study of the effect of discrete roughness elements (trips) on boundary layer transition was conducted in the NASA Langley Research Center 20-Inch Mach 6 Air Tunnel on the AFRL/ AFOSR BOLT shape. This study was intended to obtain a tripping database that could eventually be compared against experimental results from other facilities, as well as from flight. The trip locations for the present study were selected to correspond to those used for the BOLT II flight vehicle, but the heights of these discrete roughness elements were varied. Infrared thermography was used to obtain images of the effect of these trips on the behavior of the boundary layer. This report is intended as a quick release of experimental results.

## Table of Contents

Introduction.....	1
Experimental Method.....	3
Results.....	8
Summary.....	13
References.....	14
Appendix A – Run Details.....	15
Appendix B – Microscope Results.....	53

## Introduction

BOLT (an acronym for Boundary Layer Transition or Turbulence) is a sounding rocket flight experiment sponsored by the Air Force Research Laboratory (AFRL) and Air Force Office of Scientific Research (AFOSR), see Ref 1. The BOLT effort was intended as a follow-on flight project to the HIFiRE series (Ref. 2), except on a more realistic hypersonic configuration. HIFiRE 1 was a simple cone geometry, while HIFiRE 5 was an elliptic cone. BOLT is a three-dimensional shape with swept leading edges and concave surfaces (like a waverider). The intent of BOLT-related flight research is to obtain boundary layer transition or turbulence data for comparison against current techniques for analyzing and predicting boundary layer behavior. Initially, there were two separate flights funded, and both have recently flown. BOLT-1 launched out of Esrange, Sweden, during May of 2021, but was unsuccessful due to an unexpected dynamic instability that occurred soon after first stage separation. John Hopkins University Applied Physics Laboratory (JHU/APL) was the prime contractor for the first flight with the German Aerospace Center (DLR) Mobile Rocket Base (MORABA) providing launch services. BOLT-2 was successfully launched out of the NASA Wallops Flight Facility (WFF) in Virginia during March of 2022. The prime contractor for this flight was a group led by Texas A&M University (TAMU) and Calspan-University of Buffalo Research Center (CUBRC). Each flight had slightly different test objectives, which will be discussed further in the coming sections. Recently, the decision was made to fund a second attempt at the first flight, with the original team for lead and launch. This third flight (called BOLT-1B) is expected to fly from Woomera, Australia in the fall of 2024.

The BOLT geometry is shown in Fig. 1, revealing a low-curvature concave surface with swept leading edges that better represents a more realistic future hypersonic configuration (such as an airbreather), including pressure gradients and wall temperature effects. Computations to date have revealed a complex flow path that includes a center region whose boundary layer is relatively thick and stable, while the outer sections exhibit a much thinner boundary layer with a mixture of instability modes (for instance, see Ref 3). There are two, nearly identical, main surfaces (or sides) of BOLT, separated by two gutters intended to isolate the main surfaces. The two sides allow for both smooth-wall and roughness experiments to be flown at the same time. The smooth side experiment (also designated as Side A) is considered the primary purpose for the flight test, to obtain flight data on the natural processes of boundary layer transition and turbulence. For the roughness experiments (Side B), these flights provide an opportunity to examine various roughness types under hypersonic boundary layer conditions. The basic research objective of the Side B roughness experiments is to provide flight data showing roughness effects on boundary layer transition and turbulence on a realistic hypersonic vehicle. A sounding rocket flight test program provides the means to study boundary layer transition and turbulence in low disturbance environments that typically cannot be obtained in ground-based facilities. Conventional facilities can provide the proper freestream conditions, but with added noise (disturbances that alter the boundary layer instabilities), while quiet facilities can provide less noise but not at matching freestream conditions to flight (see Ref. 4). For the roughness side experiment on the BOLT-1 flight, the focus of the roughness type under investigation was two-dimensional nose-joint steps (see Ref. 5). For the BOLT-2 roughness experiment, the focus was on boundary-layer trips based on discrete roughness elements (see Ref. 6). A combined experimental and computational effort was established to inform decisions for placing and sizing these trips and laying out the sensor suite for flight. Wind tunnel data were provided by the United States Air Force Academy's (USAFA) Mach 6 Ludwig tube (M6LT) (see Ref. 7), as the NASA Langley Research Center (LaRC) 20-Inch Mach 6 Air Tunnel (see Ref. 8) was unavailable (during the early stages of the COVID-19 pandemic).



Computational mean flow solutions at wind tunnel and flight conditions were completed by TAMU to track streamlines for sensor placement and boundary layer information for scaling to flight. For both flights, LaRC was tasked with leading the definition of the roughness side experiments.

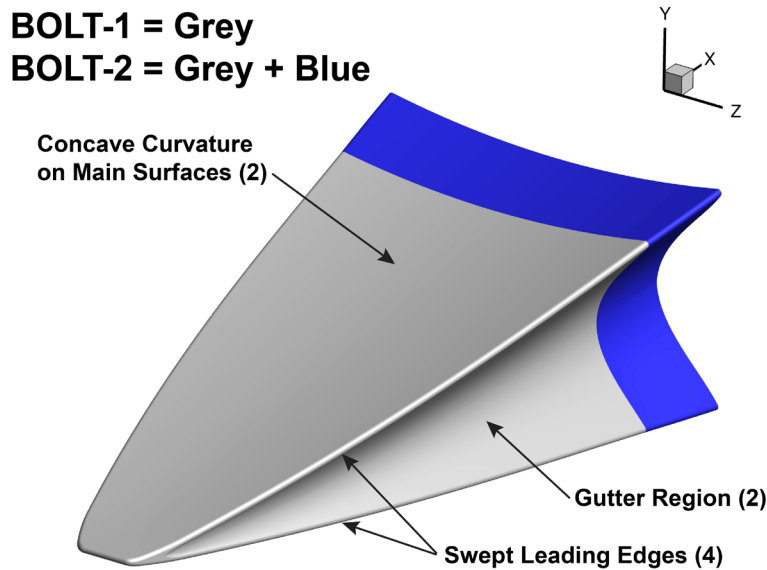


Figure 1. BOLT-1 vs. BOLT-2.

While AFRL/AFOSR has primarily sponsored the BOLT flights as university-led projects to foster the next generation of researchers in hypersonic boundary layer transition and turbulence, NASA has also been involved with both campaigns as a contributing partner with support from the Aeronautics Research Mission Directorate (ARMD), Advanced Air Vehicle Program (AAVP), Hypersonic Technologies Project (HTP). The initial set of experimental aeroheating data was obtained in the LaRC 20-Inch Mach 6 Air Tunnel on the BOLT geometry and presented at the kick-off meeting, providing an early assessment of the transition fronts and behavior (see Ref. 9). That data provided benchmark information for comparison against computational analysis being done by the broader team. Presently, there are a number of research activities underway at LaRC to provide more insight into the various mechanisms at play in support of both missions, including both experimental and computational efforts. The present paper is intended to provide a “quick release” of discrete roughness data, specifically qualitative surface infrared intensity images from which boundary layer transition onset fronts could be inferred, obtained in the 20-Inch Mach 6 Air Tunnel for comparison against results obtained elsewhere (such as in other ground-based facilities and from flight).

It should be noted that BOLT-1 and BOLT-2 are identical configurations with the exception of the length of these two flight vehicles. The BOLT-1 flight vehicle was 0.866m long and was intended to study the transition process leading to turbulence. BOLT-2 was focused more on turbulence than transition, thus there was a desire to make this second vehicle longer. An early proposed version of the BOLT-2 vehicle was a 1.5m long vehicle that became known as the Long-BOLT configuration. In the end, the as-flown BOLT-2 vehicle length was 1.0m. The present study was conducted on a Long-BOLT model, knowing that both BOLT-1 and BOLT-2 configurations were captured within its length.

## Experimental Method

### Wind Tunnel Model

The BOLT Step Test (BST) model, which was developed for testing with an infrared (IR) camera, was used for this study. The BST model, shown in Fig. 2 with most of the main components, is a half-scale model of the Long-BOLT configuration and was designed with an internal metal strongback with a polyether ether ketone (PEEK) outer surface. PEEK is a typical model material used for IR testing, as it has good surface emissivity, is inexpensive to purchase, and easily cut to shape. Note that an extra set of PEEK surfaces was built, with the second set being used for this study (modified for attaching trips). The internal metal strongback includes a nose section that could be articulated up or down with a series of inserts to create either forward-facing (FF) or rearward facing (RF) steps. For this study, steps at the nose were not the focus, instead this model was modified to include hardpoint attachments for small surface protuberances that were intended as boundary layer trips. The BST model was designed to accommodate both BOLT flight vehicles using the aforementioned Long-BOLT geometry, although only the BOLT-1 length is shown in Fig. 2. The Long-BOLT parts are an additional attachment including similar strongback and PEEK parts. The Long-BOLT model is shown in a subsequent figure. The complete list of model drawing numbers are 1299612–1299619, and 1299633–1299636.

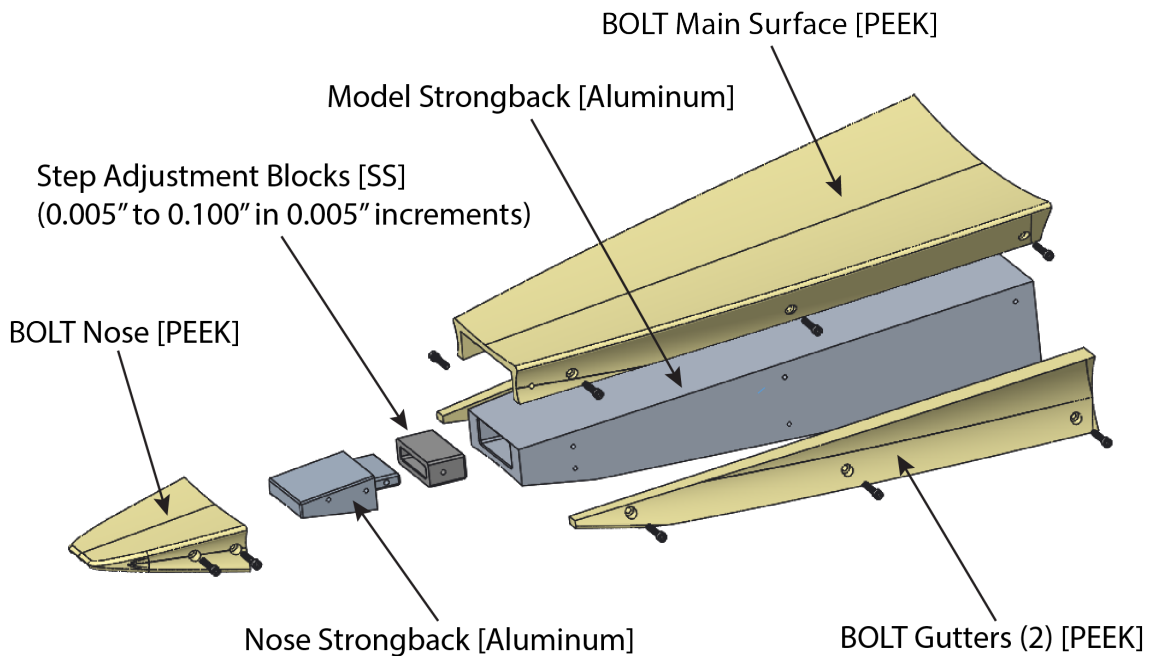


**Figure 2. Exploded view of forward section showing various model parts of the BOLT Step Test model.**

The trip locations for this study correspond to the specific sites selected for the flight of BOLT-2, with one on the vehicle centerline (CL) and two at symmetric locations near the swept leading edges (LE), as shown in Fig. 3 (along with other key features on the model). Table 1 provides these key dimensions at both vehicle and model scale. Reference **Error! Bookmark not defined.** discusses the BOLT-2 roughness side flight experiment and locations (at full scale) for these three trip sites. The extra PEEK main surface part (mentioned above) was modified with small holes drilled at the center of the trip locations with solid threaded inserts (called keenserts) installed underneath for improved holding and durability within the PEEK. Figure 4 provides a sketch of these hard-attached trips designed for this study.

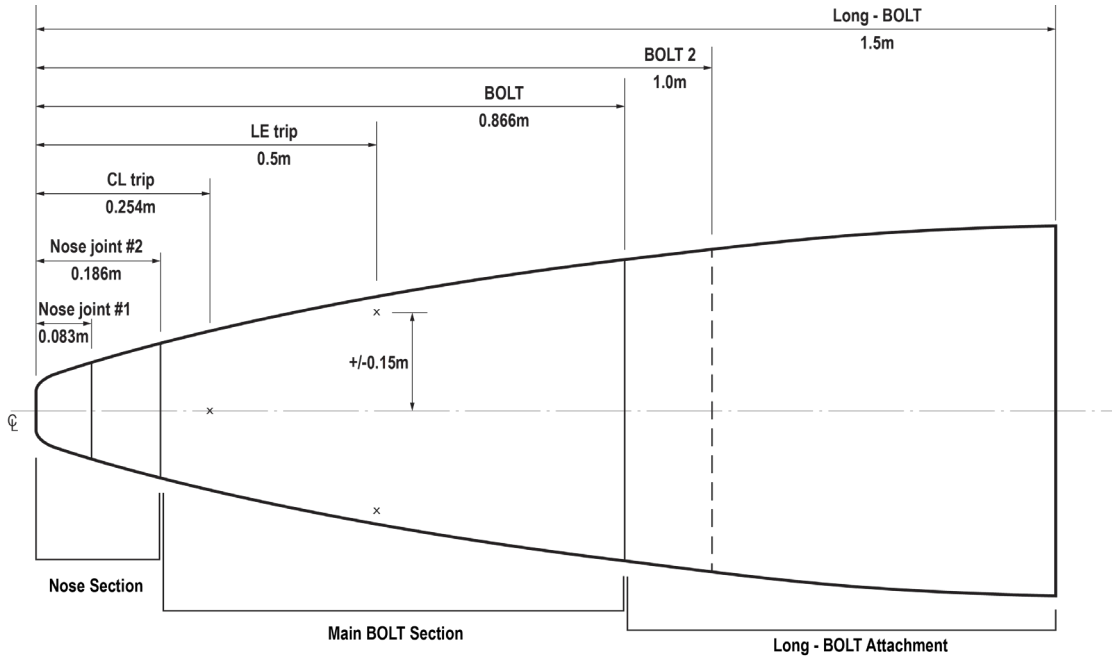


**Figure 3. Key features on the BST model based on full-scale dimensions.**

**Table 1. Key features and distances at both vehicle and model scale.**

Feature, length from origin (at nose CL)	Applicability	Full-scale length (m)	Full-scale length (in)	Model-scale length (m)	Model-scale length (in)
Joint step #1	BOLT-1 only	0.083	3.27	0.042	1.64
Joint step #2	BOLT-1 & BOLT-2	0.186	7.32	0.093	3.66
CL trip	BOLT-2 only	0.254	10.0	0.127	5.0
LE trips	BOLT-2 only	0.5/±0.15	19.7/±5.9	0.250/±0.075	9.85/±2.95
BOLT-1 length	BOLT-1 only	0.866	34.1	0.433	17.05
BOLT-2 length	BOLT-2 only	1.0	39.4	0.500	19.7
Long-BOLT length	Model only	1.5	59.1	0.750	29.5

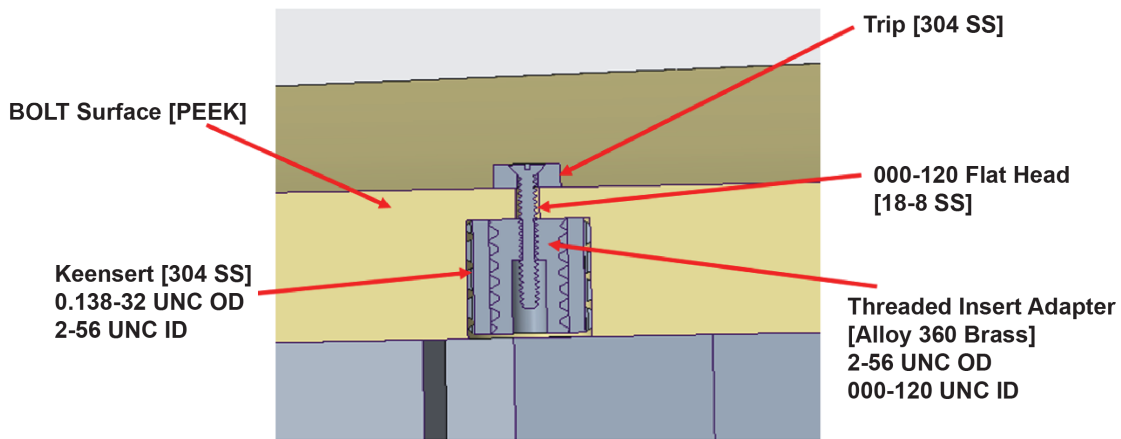


**Figure 4. Section view showing the attachment of the trips to the model.**

The model was installed in the tunnel using a strut attached to the underside of the strongback, as shown in Fig. 5. This strut was designed to place the model near the tunnel centerline. The pitch and yaw mechanism of the tunnel injection system provides the specific angle of attack and sideslip of interest for each run. For this test series, the model was held fixed at zero pitch and yaw. Also, for this study, since the focus was not step effects, a single insert block was utilized during the entire test series. Insert block -03b was chosen to provide the smallest rearward facing (RF) step based on previous experience and test results. The RF step using block -03b was measured as 0.0045" in the center and right side of the nose-joint and 0.0062 on the left side of the joint.

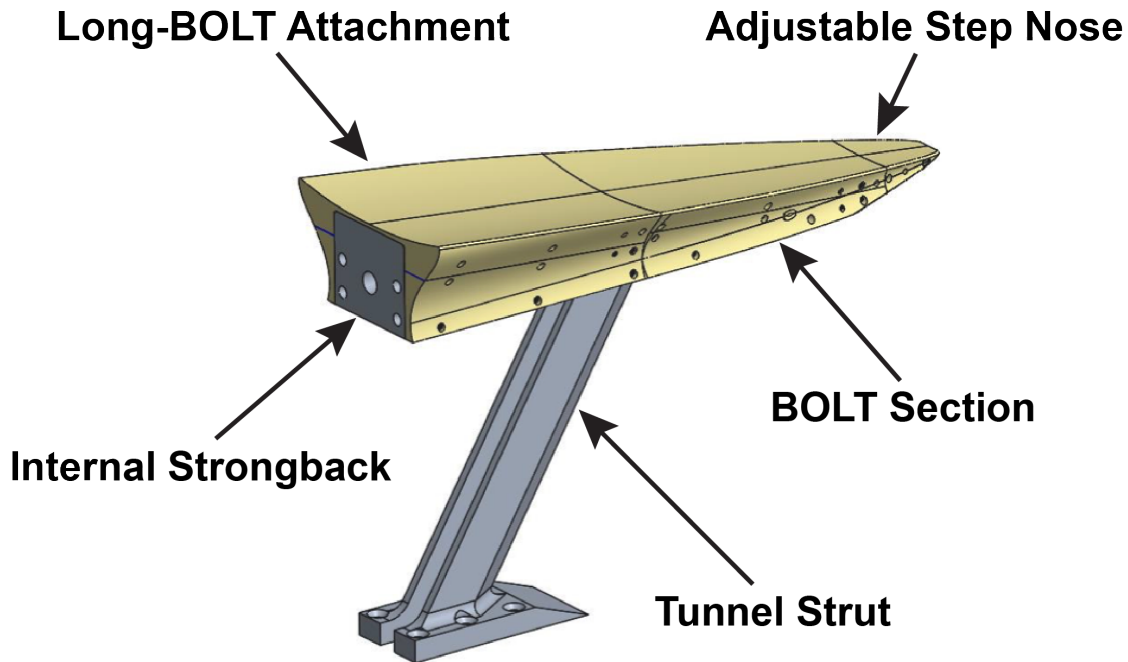


**Figure 5. Fully assembled BST model with tunnel support strut.**

The trip configuration studied here is based on the “diamond” shape, identified from the original Hyper-X trip study (see Ref. 10). The diamond configuration is shown in Fig. 6, where a square protuberance is rotated 45 deg to the flow (diagonal of the square is aligned with the freestream direction) to maximize vortex development and shedding. The key parameters for diamond trips are the trip height ( $k$ ) and square width ( $b$ ). The range of trips studied here were based on scaled versions of the dimensions and locations from the flight design (Ref. 6). Previous phosphor thermography data (unpublished) indicated that trips heights larger than the scaled flight trips were required to explore incipient, critical, and effective tripping data that were not concealed by natural transition lobes expected at moderate Reynolds numbers in this conventional noise facility. Table 2 provides the part numbers corresponding to the specific range of trip heights and widths built to support this wind tunnel study, along with a note on the intended applicability of each trip. While a range of trip heights and widths were fabricated, only select combinations that represented the scaled flight trips with increments taller were tested during this entry, as defined by Table 3, which also provides the measured heights as derived from surface scans (see Appendix B). Trip configuration 1 represents the scaled trip heights and widths corresponding to the BOLT-2 flight geometry with the -4 part on the model centerline (CL) and two -11 parts on both leading edges (LE). Trip configurations 2–4 get incrementally

taller. Note that the two smallest trips at the LE (parts -1 and -11) were measured to be higher than expected, due to the screw head protruding slightly above the trip during scans (not seen by eye, but captured by these measurements). The length of the screws available were bottoming out for the smaller trips such that the screw heads were forced to protrude slightly. Since it appeared that these cases were not that critical due to the natural transition behavior, there was no attempt made to correct and/or rescan these two cases.

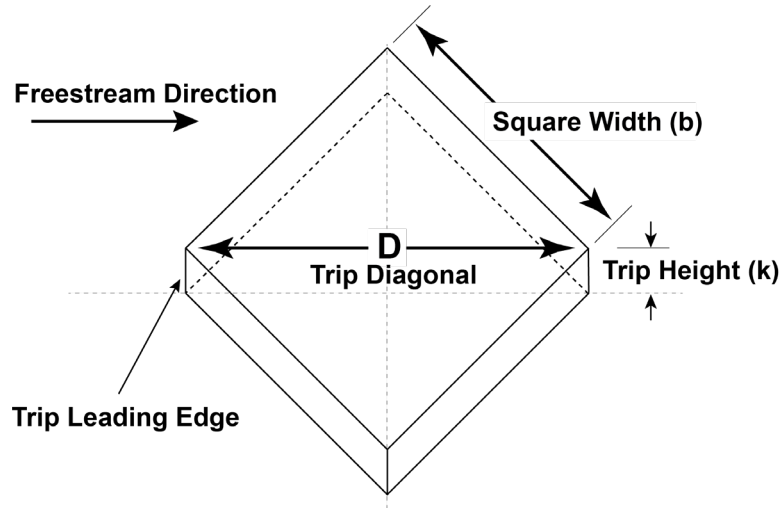


Figure 6. Oblique view of trips showing orientation and key dimensions.

Table 2. Trip parts built for this study.

PART NUMBER	Desired Trip Height (k) (in)	Desired Trip Width (b) (in)	Notes
300931-1	0.026	0.052	LE, nominal +1
300931-2	0.026	0.156	CL, nominal -1
300931-3	0.052	0.052	LE, nominal +2
300931-4	0.052	0.156	CL, nominal
300931-5	0.076	0.052	LE, nominal +3
300931-6	0.076	0.156	CL, nominal +1
300931-7	0.100	0.052	LE, nominal +4
300931-8	0.100	0.156	CL, nominal +2
300931-9	0.124	0.052	LE, nominal +5
300931-10	0.124	0.156	CL, nominal +3
300931-11	0.018	0.052	LE, nominal

Table 3. Trip configurations utilized during testing.

Trip Configs	CL Part #	Measured Height (in)	LE Part #	Measured Height (in)
1 (flight scaled)	-4	0.052	-11	<b>0.021</b>
2 (+1 bigger)	-6	0.076	-1	<b>0.031</b>
3 (+2 bigger)	-8	0.100	-3	0.052
4 (+3 bigger)	-10	0.124	-5	0.077

## Tunnel

The NASA LaRC 20-Inch Mach 6 Air Tunnel is a blowdown facility in which heated, dried, and filtered air is used as the test gas. The tunnel has a two-dimensional contoured nozzle that opens into a 20.5-in by 20.0-in test section and is equipped with a bottom-mounted injection system that can transfer a model from a sheltered position within the injection box to tunnel centerline in less than 0.5 sec. The injection system provides a pitch range of -5 to +55 degrees and a yaw range of  $\pm 5$  degrees. Run times of up to 15 minutes are possible in this facility, although for the current aeroheating study, run times of only a few seconds were required. The nominal reservoir conditions of this facility produce perfect-gas freestream flows with Mach numbers between 5.8 and 6.1 and unit Reynolds numbers of  $0.34 \times 10^6/\text{ft}$  to  $7.89 \times 10^6/\text{ft}$ . This range of Reynolds numbers is capable of producing laminar, transitional, or turbulent flow on most model geometries, and thus is primarily used for heat-transfer and boundary-layer transition studies. A recent report on measurements of the freestream noise content of this conventional type facility is provided in Ref. 11. The facility is part of the Langley Aerothermodynamics Laboratory (LAL) and is operated by staff in the Supersonic/Hypersonic Testing Branch of the Research Directorate. This study was designated by LAL as test 7071 and the run matrix is provided in Appendix A.

## Data Acquisition

The primary test technique for this study was infrared (IR) thermography using a FLIR SC6701s long-wave IR camera with 50mm lens. The IR camera was mounted above the tunnel and views the model through a large Zinc Selenide (ZnSe) window, with antireflective coating (ideal for LWIR wavelengths from 8 – 12  $\mu\text{m}$ ). The IR camera captured both prerun images of the model (at ambient room temperature conditions) and a series of run images (after the tunnel was started and model injected) to monitor the surface heating in time. These images would normally be used to compute one-dimensional heat transfer in a manner similar to that used for our standard phosphor thermography system (IHEAT). For this quick release document, only representative raw images in IR intensity counts for each run are provided as the tunnel-specific camera/window calibrations and heat transfer data reduction methodology are still under development. Figure 7 provides a sketch showing the camera field of view and subsequent image cropping done for this report. The IR camera framing rate and tunnel flow conditions are synced at 60 fps. The images captured for this report were selected as frame 300, or 5 seconds after the model reached tunnel centerline. Several thermocouples were attached to underside locations on the model to monitor the bulk model temperatures throughout the test series. These thermocouples were attached to both the internal model strongback and the PEEK parts as a check of the prerun temperatures and to insure no residual heat was building up in the model between runs.

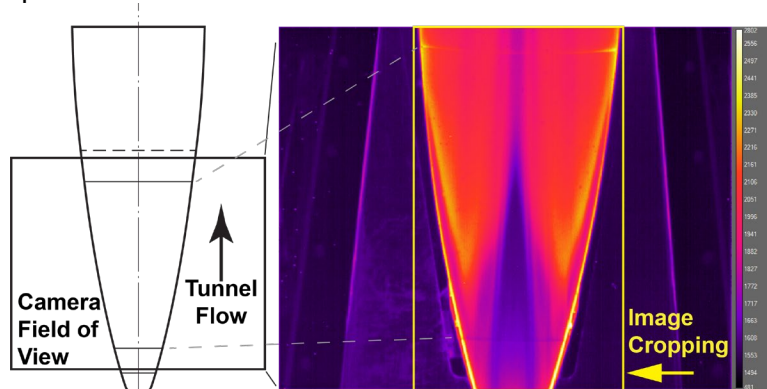


Figure 7. Camera view of Long-BOLT model.

## Results

This section is intended to provide a review of the trends observed from the data, first starting with the Reynolds number sweep of the baseline no-trip case and then looking at progressively bigger trips. As mentioned before, the images contained within these figures are the raw results in IR intensity counts (they have not been converted to temperature or heating yet). All test data, in run sequential order, are captured in Appendix A. The run log for the test is also included in Appendix A, which includes the measured flow conditions for each run. The observations of the onset of boundary layer transition in the following discussion are subjectively identified based on the authors engineering judgement.

The Reynolds number sweep for the baseline/no-trip cases are shown in Fig. 8. At the lower freestream unit Reynolds numbers (below 0.8 million/ft),\* the observable area remains fully laminar with a darker (low heating) center region where the boundary layer is relatively thick. Away from the center region, the lighter colors are indicative of higher heating associated with a thinner boundary layer (BL). Faint streaks (shown by a sample image in Fig. 9) are observed within these outer thin BL regions, which are attributable to observations of known boundary layer instability modes. As Reynolds number increases (above 0.8 million/ft), transition onset is seen (the light pink to red colors) near the back of the model which systematically progresses forward in a symmetric fashion (onset lobes on either side of CL). At the highest Reynolds number case (4.1 million/ft) the transition lobes have pushed significantly forward covering a large portion of the model. It is important to note that these BL transition lobes are more prominent in this “conventional” type hypersonic facility, than they would be in quiet tunnels or in flight.

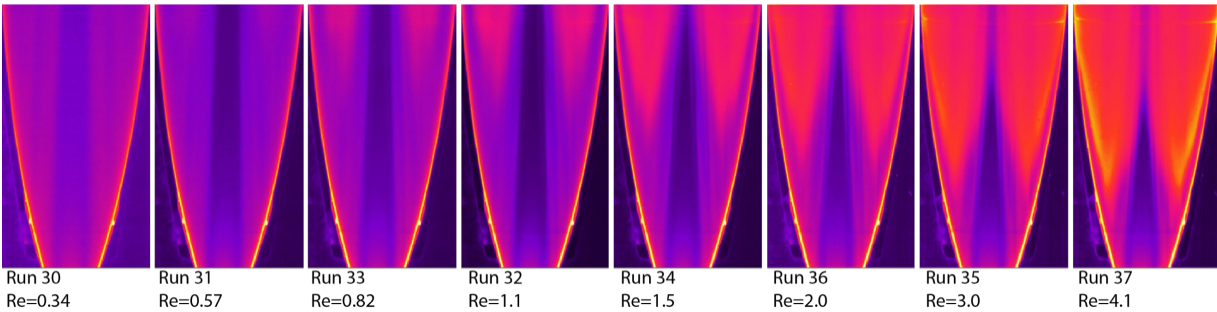


Figure 8. Baseline Results.

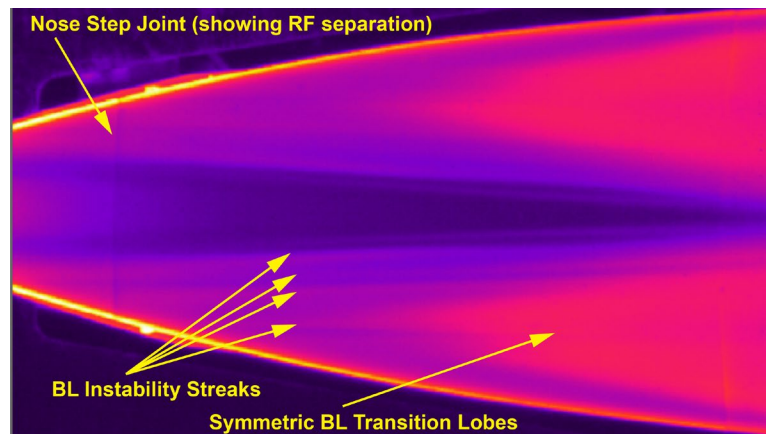
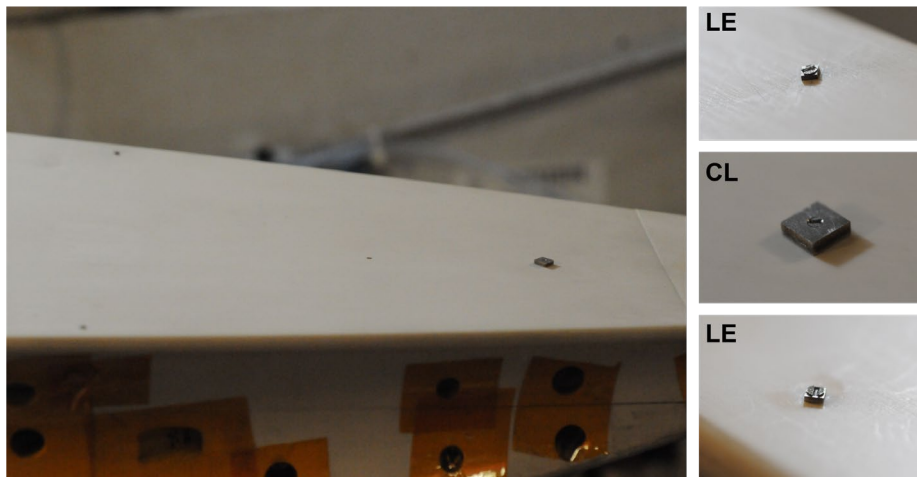


Figure 9. Sample IR intensity image indicating key BL features.

\* Note: figures utilize shorthand of Re for unit Reynolds number based on million/ft.

For the entire test series, the same nose step insert (-03b) was installed and never adjusted until the steps could again be scanned after the test. These posttest scans of the nose joints and as-installed trips are captured in Appendix B. Close scrutiny of the higher Reynolds number cases above show a very thin darker line (more clearly seen in Fig. 9), indicating the location of the nose joint. The dark line indicates a small separation region just behind the RF step. Previous testing (not shown here and not yet published) with forward facing (FF) steps provided a bright line at the nose joint, directly the result of the increased heating at the joint.

Figure 10 provides photos of the flight-scaled trips (designated as trip configuration #1, based on -4 trip at the CL and -11 trips at the LE locations). IR results for this trip configuration are provided in Fig. 11. The CL trip is seen to promote a disturbance (or streak) that dissipates at the lower Reynolds numbers (left two images), but then develops into a turbulent wedge (i.e., localized region of increasing heating above the laminar levels) at Re of 1.5 million/ft and higher. This would suggest that incipient transition for this trip size and location occurs for unit Reynolds numbers somewhere between 1.1 and 1.5 million/ft. This result is consistent with the previous results obtained in the USAFA tunnel, which was used to select the trip heights for the flight of BOLT-2. Moving to the LE trips, the downstream behavior from these locations are harder to interpret, unfortunately. Disturbances are seen, for all five Re cases, coming from the LE locations, but the progression of the natural lobes, as Reynolds number increases, obscures any interpretation of when an incipient condition is reached for this location and size. This was the primary reason for selecting a series of trips larger than the scaled flight cases for this study, to probe incipient results at the LE locations at lower Reynolds numbers where the natural lobes should not be present.



**Figure 10. Photos showing trip configuration #1 [Source: NASA].**

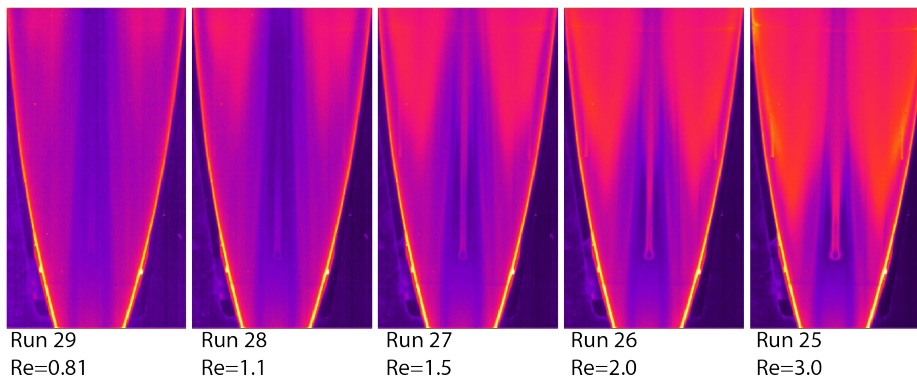


**Figure 11. Trip #1 Results.**



Photos of the installed trips for configuration #2 (CL-6 and LE-1) are provided in Fig. 12, while IR images for the series of runs with this trip configuration are shown in Fig. 13 (for the same Reynolds number sweep as before). Since the trip heights have increased, one would expect transition onset at a lower Reynolds number than the previous case. First, looking at the CL case, the streak seen behind the trip does produce a noticeable increase in heating (interpreted as the development of the turbulent wedge) by  $Re = 1$  million/ft (earlier than for trip case #1), which is identified as the incipient transition point for this trip size (and location). Next, looking at the LE trips, the streaks are more pronounced than before but still get lost in the natural lobes as Reynolds number increases. Since the IR data were not able to clearly identify an onset point for this LE trip (and also the prior case), there did not seem to be a need to clarify the actual trip height from the scanned data of Appendix B (where the measured values were taller than expected). Note that Appendix A includes all IR images shown in the discussion section at a bigger size.

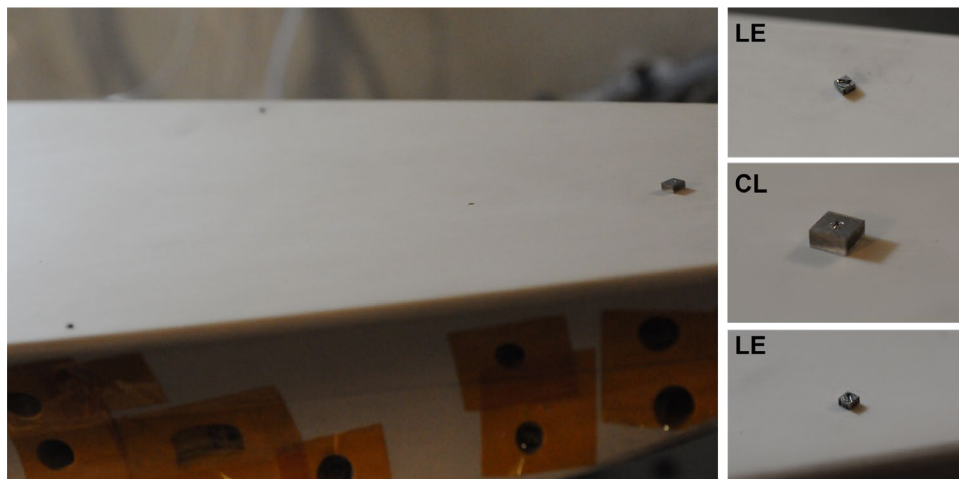


**Figure 12. Photos showing trip configuration #2 [Source: NASA].**

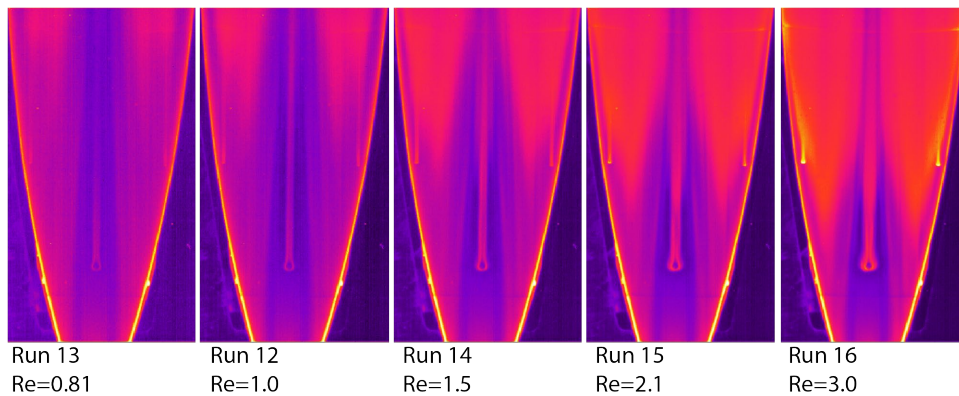


**Figure 13. Trip #2 results.**

Photos of the three trips used for configuration #3 (CL-8 and LE-3) are provided in Fig. 14, and the subsequent IR results shown in Fig. 15. This is the first trip case in which transition onset can possibly be seen from the data for both the CL and LE cases. First looking at the CL trip, the wake disturbance appears more prominent (and may be even spreading laterally) at  $Re = 0.8$  million/ft, and thus is identified as the incipient point for this case. Next, looking at the LE trips, the wake disturbance is also more prominent at the same Reynolds number, perhaps indicating an incipient condition, although the natural lobes are also starting to appear at this Reynolds number, which complicates a definitive declaration here.



**Figure 14. Photos showing trip configuration #3 [Source: NASA].**

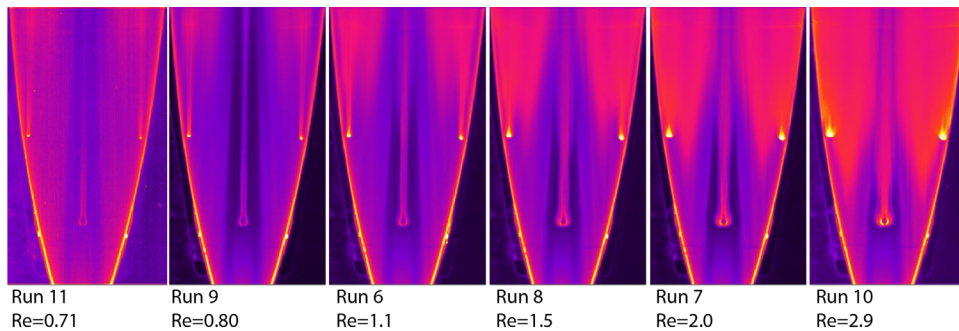


**Figure 15. Trip #3 results.**

Photos of the tallest trip case tested here, trip configuration #4 (CL-10 and LE-5), are provided in Fig. 16, while the IR results are shown in Fig. 17. For the CL location, the trip appears incipient somewhere between  $Re$  of 0.58 and 0.82 million/ft. When comparing this height to the previous case, the downstream wedge that forms at  $Re = 0.82$  million/ft is broader and more pronounced, which suggests an earlier incipient point here. Looking at the LE trips, the wedges do become pronounced before the natural lobes form, thus suggesting incipient behavior by  $Re=0.58$  million/ft.

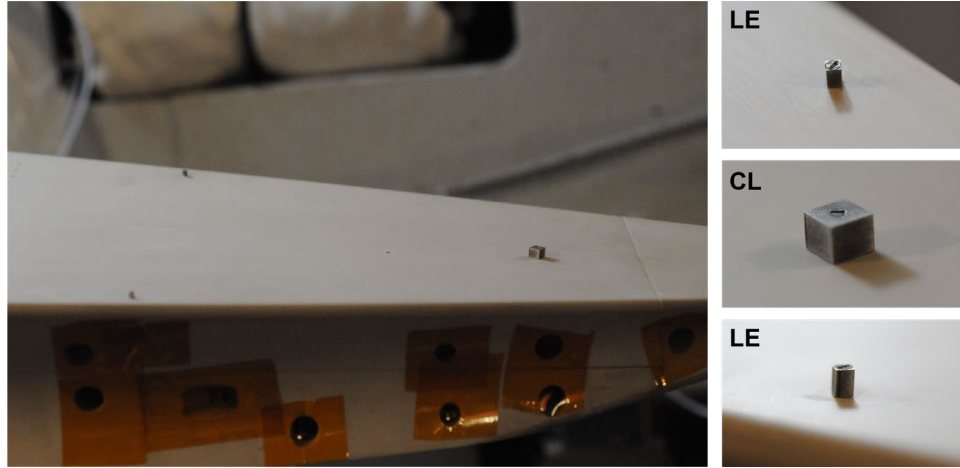


**Figure 16. Photos showing trip configuration #4 [Source: NASA].**

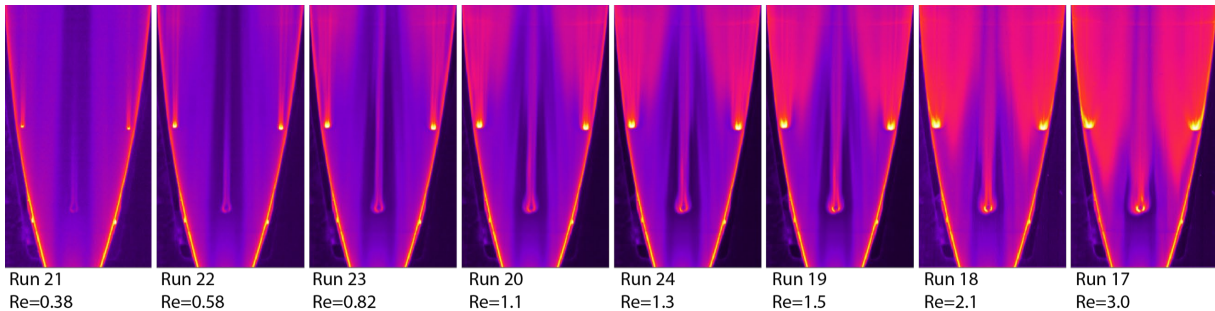


**Figure 17. Trip #4 results.**

One final comment from these experimental results with the largest trips near the LE is that the disturbance path under laminar conditions appears to be straight back from the trip, which is consistent with the unpublished observations that were made from the USAFA test entry. The flight instrumentation layout had been previously selected to be directly behind the trip locations based on these earlier results. Preliminary computations completed after the instrumentation locations had been finalized had suggested that the disturbance path might curve outboard.

## Summary

This document is intended as a quick release report for Test 7071 in the NASA Langley 20-Inch Mach 6 Air Tunnel, which was conducted to examine boundary layer trips on the BOLT configuration, specifically on the half-scale BOLT Step Test model. The intent of this study was to provide experimental infrared intensity images that could be used to examine discrete roughness BLT correlations for comparison against other ground-based data and flight. The trip locations utilized for this test are consistent with locations selected for the BOLT-2 flight vehicle. The trip heights were the primary test variable examined during this entry. IR thermography was used to obtain surface radiance images, from which the boundary layer behavior is inferred for each run. Due to the quick release nature of this report, analysis of results is kept to a minimum, mainly a description of the qualitative trends associated with the range of tested trip sizes, such as the incipient conditions identified for each trip case.

## References

---

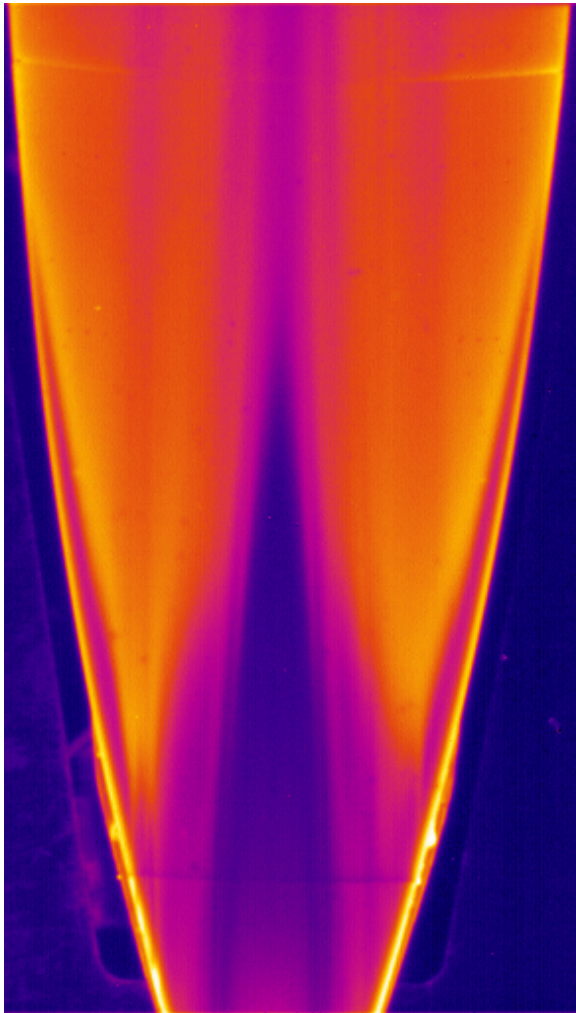
1. Wheaton, B.M., Berridge, D.C., Wolf, T.D., Stevens, R.T., and McGrath, B.E., "Boundary Layer Transition (BOLT) Flight Experiment Overview," AIAA Paper 2018-2892.
2. Dolvin, D. J., "Hypersonic International Flight Research and Experimentation (HIFiRE) Fundamental Sciences and Technology Development Strategy," AIAA Paper 2008-2581.
3. Johnston, Z. M., and Candler, G. V., "Hypersonic Simulations of the BOLT-2 Subscale Geometry," AIAA Paper 2021-0365.
4. Schneider, S. P., "Development of Hypersonic Quiet Tunnels," *Journal of Spacecraft and Rockets* Vol. 45, No. 4, July-Aug 2008, pp. 641-664. DOI: 10.2514/1.34489
5. Berry, S.A., Wheaton, B.M., and Chynoweth, B.C., "Secondary Side Considerations for the BOLT Flight Experiment," AIAA Paper 2020-1559.
6. Berry, S.A., Semper, M.T., Riha, A.K, Mullen, C.D., Reed, H.L., Dufrene, A.T., and Fasel, H.F., "Development of the BOLT II Roughness Experiment for Flight," AIAA Paper 2022-0347.
7. Cummings, R. M. and McLaughlin, T. E., "Hypersonic Ludwig Tube Design and Future Usage at the US Air Force Academy," AIAA Paper 2012-0734. DOI: 10.2514/6.2012-734
8. Berger, K., Rufer, S., Hollingsworth, K., and Wright, S., "NASA Langley Aerothermodynamic Laboratory: Hypersonic Testing Capabilities," AIAA Paper 2015-1337.
9. Berry, S. A., Mason, M. L., Greene, F. A., King, R. A., Rieken, E. F., and Basore, K.D., "LaRC Aerothermodynamic Ground Tests in Support of BOLT Flight Experiment," AIAA Paper 2019-0091.
10. Berry, S. A.; Auslender, A. H.; Dille, A. D.; and Calleja, J. F., "Hypersonic Boundary-Layer Trip Development for Hyper-X," *Journal of Spacecraft and Rockets*, Vol. 38, No. 6, 2001, pp. 853-864.
11. Chou, A., Leidy, A. N., Bathel, B. F., King, R. A., and Herring, G. C., "Measurements of Freestream Fluctuations in the NASA Langley 20-Inch Mach 6 Tunnel," AIAA Paper 2018-3073.

Appendix A - Compilation of Run Details

Appendix A

Date	Time	Run	Model	View	Set Conditions		Measured Conditions			Strut		Model			Nose	Comments
					Pt1	Tt1	Pt1	Tt1	Re/ft	Alpha	Psi	$\alpha$	$\beta$	$\phi$		
					{psia}	{deg F}	{psia}	{deg F}	{1/ft}	{deg}	{deg}	{deg}	{deg}	{deg}		
9 Jun 22	7:38	1	IR-03b	Wind	250	450	253.74	450.04	4.08	0.00	0.00	0.00	0.00	0.00	0.0902	72.0F / Insert -03b used for all
9 Jun 22	8:10	2	IR-03b	Wind	125	450	124.92	450.27	2.04	0.00	0.00	0.00	0.00	0.00	0.0902	75.0F
9 Jun 22	8:42	3	IR-03b	Wind	475	425	475.43	429.99	7.89	0.00	0.00	0.00	0.00	0.00	0.0902	75.5F
9 Jun 22	10:00	4	IR-03b	Wind	60	420	59.73	417.19	1.06	0.00	0.00	0.00	0.00	0.00	0.0902	75.0F
9 Jun 22	10:30	5	IR-03b	Wind	250	450	253.09	452.38	4.06	0.00	0.00	0.00	0.00	0.00	0.0902	76.0F
9 Jun 22	12:21	6	CL -8; LE - 3	Wind	60	420	60.00	419.69	1.06	0.00	0.00	0.00	0.00	0.00	0.0902	75.0F
9 Jun 22	12:52	7	CL -8; LE - 3	Wind	125	450	125.30	450.10	2.04	0.00	0.00	0.00	0.00	0.00	0.0902	76.0F
9 Jun 22	13:32	8	CL -8; LE - 3	Wind	90	440	89.25	438.89	1.50	0.00	0.00	0.00	0.00	0.00	0.0902	76.5F
9 Jun 22	14:32	9	CL -8; LE - 3	Wind	45	410	43.68	408.40	0.80	0.00	0.00	0.00	0.00	0.00	0.0902	77.5F
10 Jun 22	8:55	10	CL -8; LE - 3	Wind	180	450	181.38	449.87	2.94	0.00	0.00	0.00	0.00	0.00	0.0902	75.0F
10 Jun 22	10:55	11	CL -8; LE - 3	Wind	30	410	36.61	385.66	0.71	0.00	0.00	0.00	0.00	0.00	0.0902	76.5F
10 Jun 22	12:15	12	CL -6; LE - 1	Wind	60	420	58.99	418.58	1.05	0.00	0.00	0.00	0.00	0.00	0.0902	77.0F
10 Jun 22	13:10	13	CL -6; LE - 1	Wind	45	410	44.36	407.80	0.81	0.00	0.00	0.00	0.00	0.00	0.0902	77.5F
10 Jun 22	13:40	14	CL -6; LE - 1	Wind	90	440	89.44	438.27	1.51	0.00	0.00	0.00	0.00	0.00	0.0902	77.5F
10 Jun 22	14:06	15	CL -6; LE - 1	Wind	125	450	125.76	448.52	2.06	0.00	0.00	0.00	0.00	0.00	0.0902	77.5F
10 Jun 22	14:35	16	CL -6; LE - 1	Wind	180	450	183.82	448.06	2.98	0.00	0.00	0.00	0.00	0.00	0.0902	78.5F
13 Jun 22	7:40	17	CL -10; LE - 5	Wind	180	450	182.95	448.96	2.97	0.00	0.00	0.00	0.00	0.00	0.0902	72.5F
13 Jun 22	8:10	18	CL -10; LE - 5	Wind	125	450	125.01	447.18	2.05	0.00	0.00	0.00	0.00	0.00	0.0902	74.5F
13 Jun 22	9:00	19	CL -10; LE - 5	Wind	90	440	89.81	438.01	1.51	0.00	0.00	0.00	0.00	0.00	0.0902	74.5F
13 Jun 22	10:40	20	CL -10; LE - 5	Wind	60	420	59.68	417.58	1.06	0.00	0.00	0.00	0.00	0.00	0.0902	73.0F
13 Jun 22	12:15	21	CL -10; LE - 5	Wind	15	360	17.49	345.25	0.38	0.00	0.00	0.00	0.00	0.00	0.0902	73.0F
13 Jun 22	13:00	22	CL -10; LE - 5	Wind	30	410	29.48	385.98	0.58	0.00	0.00	0.00	0.00	0.00	0.0902	73.0F
13 Jun 22	13:40	23	CL -10; LE - 5	Wind	45	410	44.88	408.06	0.82	0.00	0.00	0.00	0.00	0.00	0.0902	74.5F
13 Jun 22	14:10	24	CL -10; LE - 5	Wind	75	425	73.68	434.95	1.26	0.00	0.00	0.00	0.00	0.00	0.0902	74.5F
15 Jun 22	7:40	25	CL -4; LE - 11	Wind	180	450	182.35	448.68	2.96	0.00	0.00	0.00	0.00	0.00	0.0902	72.5F
15 Jun 22	8:20	26	CL -4; LE - 11	Wind	125	450	124.60	448.17	2.04	0.00	0.00	0.00	0.00	0.00	0.0902	74.0F/ No prerun maceu
15 Jun 22	9:00	27	CL -4; LE - 11	Wind	90	440	89.03	439.02	1.50	0.00	0.00	0.00	0.00	0.00	0.0902	74.5F
15 Jun 22	9:57	28	CL -4; LE - 11	Wind	60	420	64.05	423.96	1.12	0.00	0.00	0.00	0.00	0.00	0.0902	77.5 F
15 Jun 22	10:50	29	CL -4; LE - 11	Wind	45	410	44.38	407.50	0.81	0.00	0.00	0.00	0.00	0.00	0.0902	76.5F
15 Jun 22	12:23	30	Baseline	Wind	15	360	15.68	356.65	0.34	0.00	0.00	0.00	0.00	0.00	0.0902	77.0 F
15 Jun 22	12:52	31	Baseline	Wind	30	410	29.73	400.58	0.57	0.00	0.00	0.00	0.00	0.00	0.0902	77.0F
15 Jun 22	13:26	32	Baseline	Wind	60	420	59.70	421.11	1.05	0.00	0.00	0.00	0.00	0.00	0.0902	78.5F
15 Jun 22	13:41	33	Baseline	Wind	45	410	44.96	408.42	0.82	0.00	0.00	0.00	0.00	0.00	0.0902	78.5F
15 Jun 22	14:28	34	Baseline	Wind	90	440	90.10	438.80	1.52	0.00	0.00	0.00	0.00	0.00	0.0902	78.0F
17 Jun 22	7:50	35	Baseline	Wind	180	450	182.05	448.63	2.95	0.00	0.00	0.00	0.00	0.00	0.0902	73.0F
17 Jun 22	8:30	36	Baseline	Wind	125	450	124.10	447.62	2.03	0.00	0.00	0.00	0.00	0.00	0.0902	73.0F
17 Jun 22	9:40	37	Baseline	Wind	250	450	253.24	450.88	4.07	0.00	0.00	0.00	0.00	0.00	0.0902	75.5F

## Test 7071 Run 1

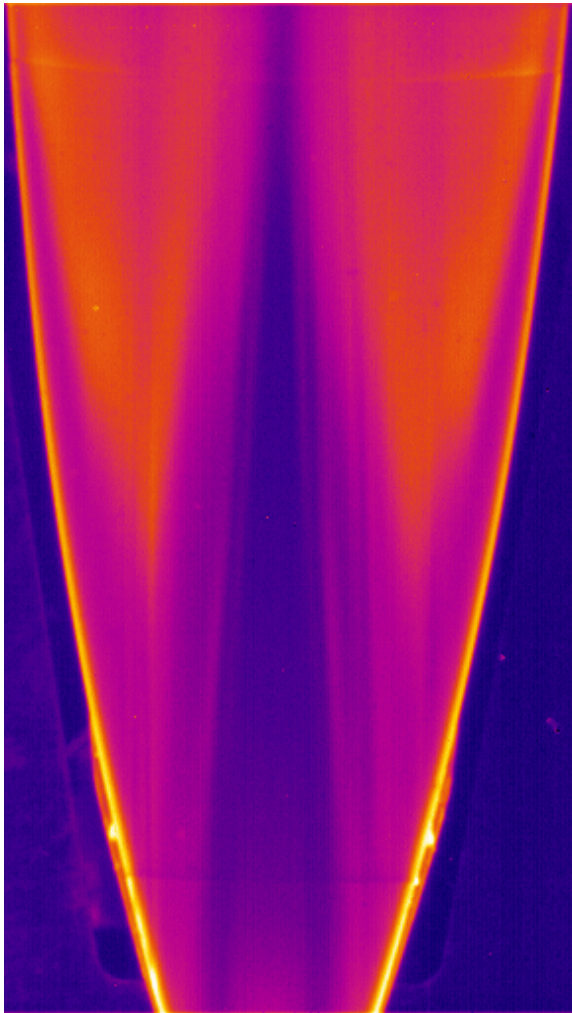


Trip configuration: Baseline  
Unit Re: 4.08 Million/ft  
Re-L  
Alpha = 0.0 deg  
Mach = 5.9  
Tunnel set conditions:  
Pt1 = 253.7 psi  
Tt1 = 450.4 °F

No trips  
Baseline, for comparison to previous data

Sample IR intensity image at  $t=5$  seconds (image 300)

## Test 7071 Run 2



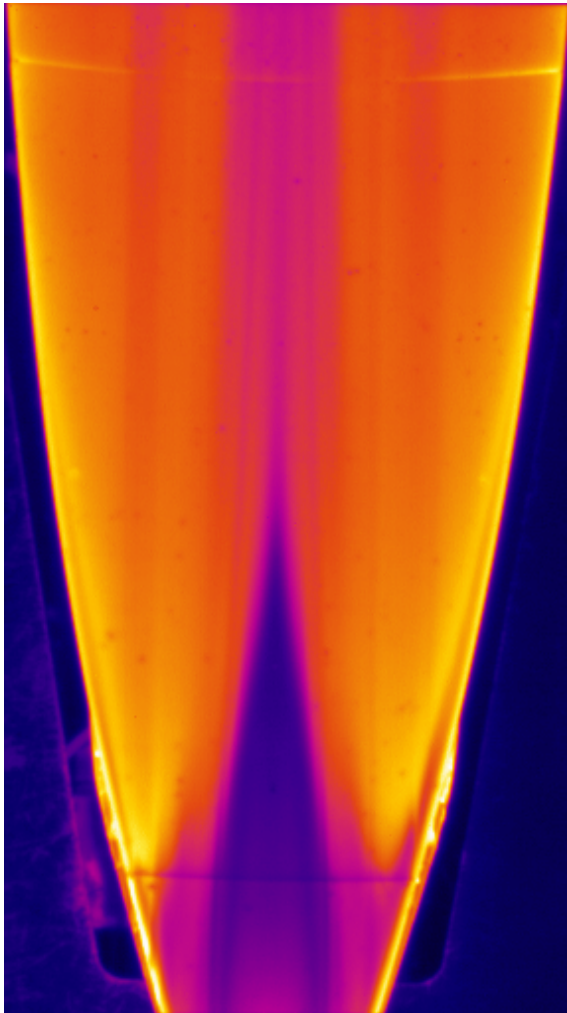
Trip configuration: Baseline  
Unit Re: 2.04 Million/ft  
Re-L  
Alpha = 0.0 deg  
Mach = 5.9  
Tunnel set conditions:  
Pt1 = 124.9 psi  
Tt1 = 450.3 °F

No trips  
Baseline, for comparison to previous data

Sample IR intensity image at t=5 seconds (image 300)



### Test 7071 Run 3

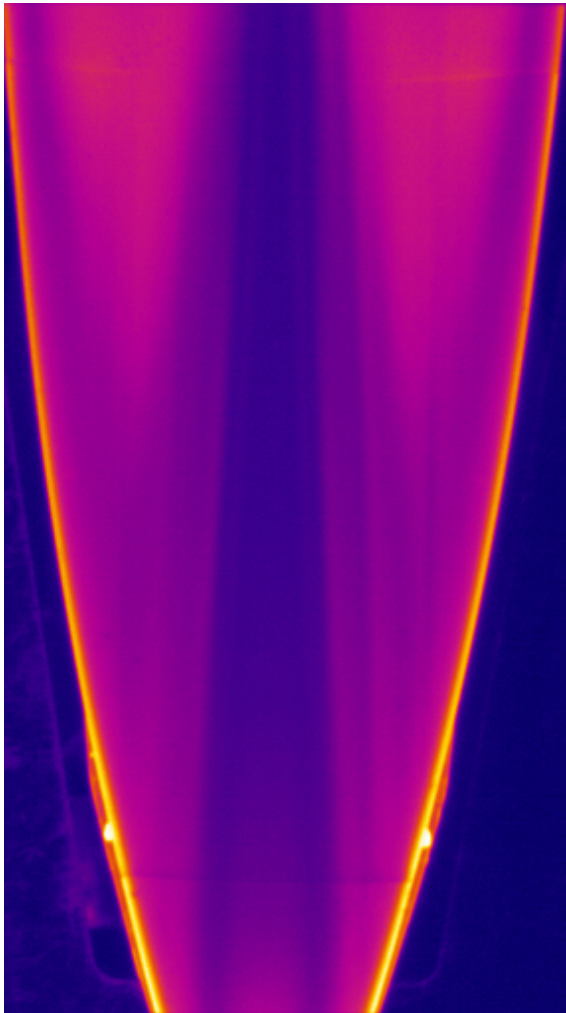


Trip configuration: Baseline  
Unit Re: 7.89 Million/ft  
Re-L  
Alpha = 0.0 deg  
Mach = 5.9  
Tunnel set conditions:  
Pt1 = 475.4 psi  
Tt1 = 430.0 °F

No trips  
Baseline, for comparison to previous data

Sample IR intensity image at t=5 seconds (image 300)

## Test 7071 Run 4

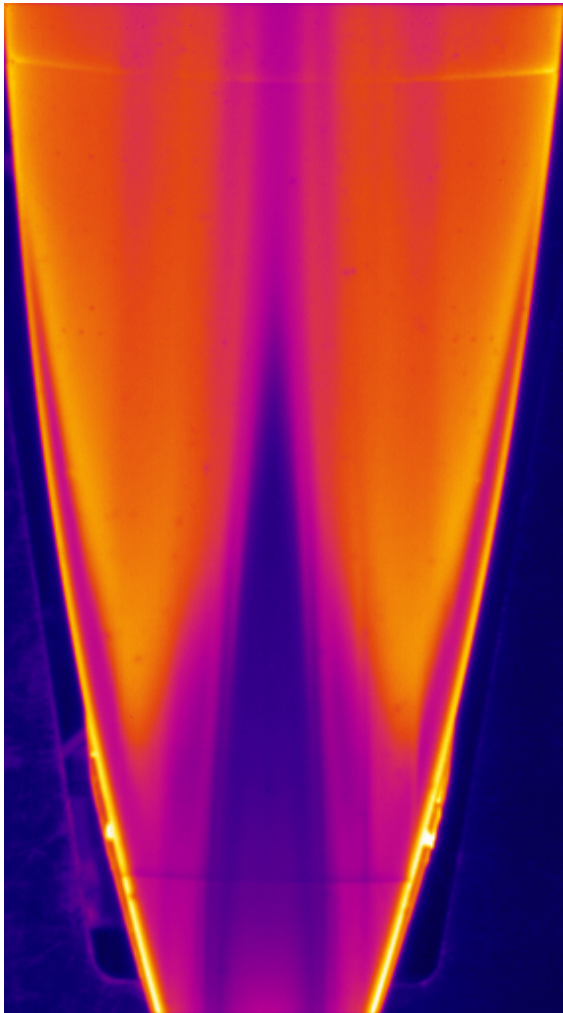


Trip configuration: Baseline  
Unit Re: 1.06 Million/ft  
Re-L  
Alpha = 0.0 deg  
Mach = 5.9  
Tunnel set conditions:  
Pt1 = 59.7 psi  
Tt1 = 417.2 °F

No trips  
Baseline, for comparison to previous data

Sample IR intensity image at  $t=5$  seconds (image 300)

## Test 7071 Run 5

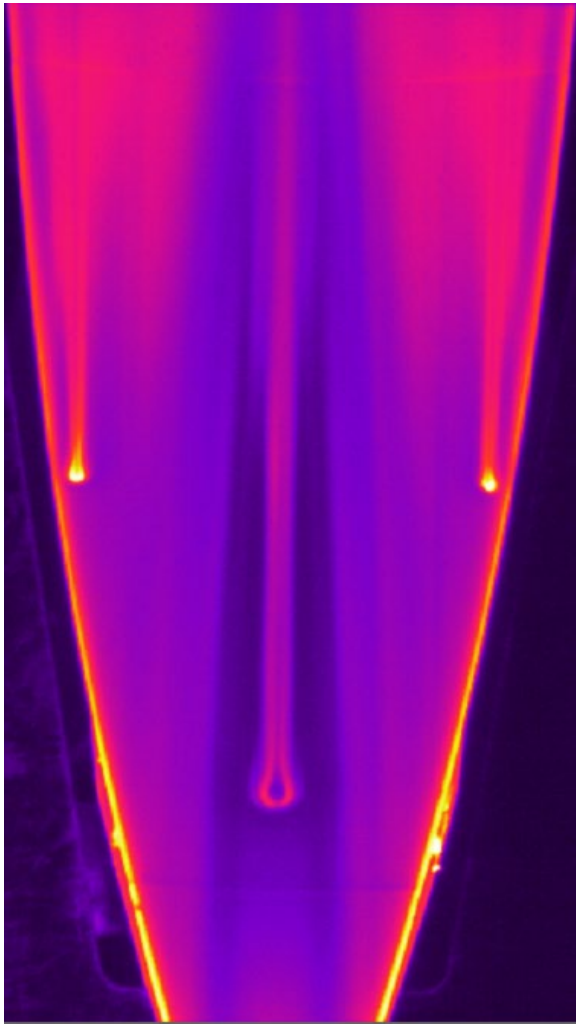


Trip configuration: Baseline  
Unit Re: 4.06 Million/ft  
Re-L  
Alpha = 0.0 deg  
Mach = 5.9  
Tunnel set conditions:  
Pt1 = 253.1 psi  
Tt1 = 452.4 °F

No trips  
Baseline, for comparison to previous data

Sample IR intensity image at  $t=5$  seconds (image 300)

## Test 7071 Run 6



Trip configuration: CL-8; LE-3  
Unit Re: 1.06 Million/ft  
Re-L  
Alpha = 0.0 deg  
Mach = 5.9  
Tunnel set conditions:  
Pt1 = 60.2 psi  
Tt1 = 419.7 °F

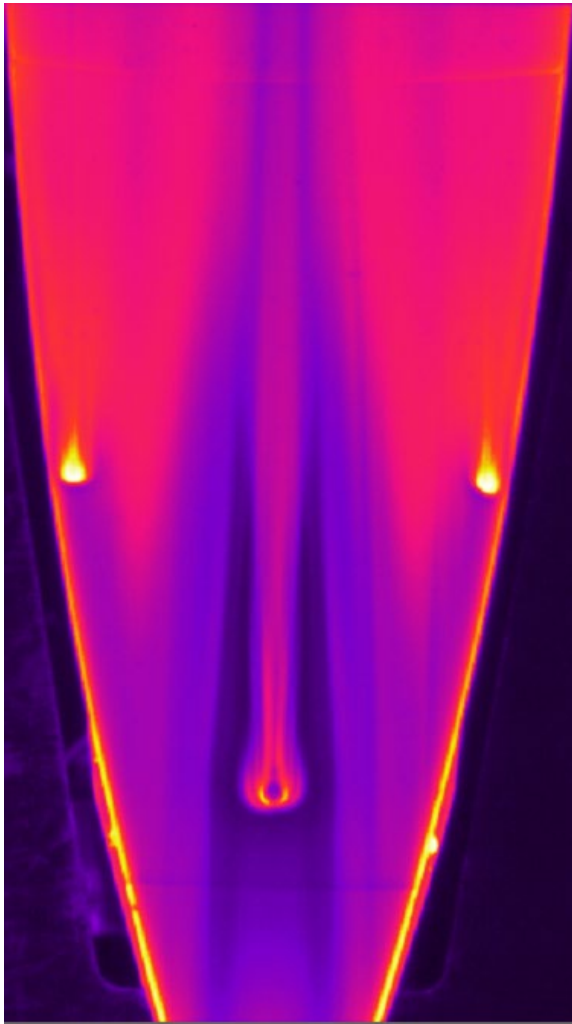
Measured trip dimensions?  
CL #8  
k=0.100"  
b=0.156"

LE #3  
k=0.052"  
b=0.052"

Local conditions at trips?

Sample IR intensity image at t=5 seconds (image 300)

## Test 7071 Run 7



Trip configuration: CL-8; LE-3  
Unit Re: 2.04 Million/ft  
Re-L  
Alpha = 0.0 deg  
Mach = 5.9  
Tunnel set conditions:  
Pt1 = 125.3 psi  
Tt1 = 450.1 °F

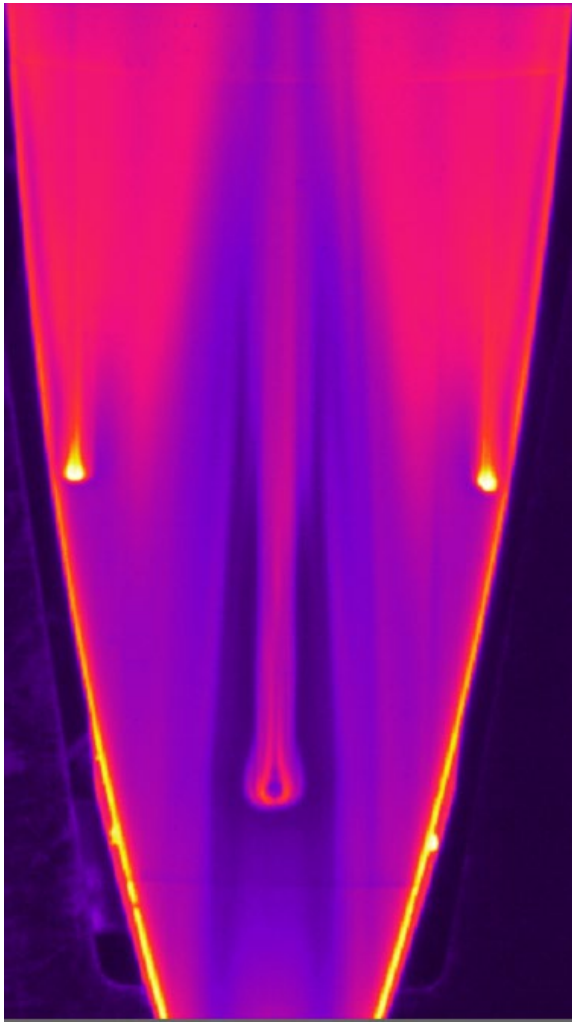
Measured trip dimensions?  
CL #8  
k=0.100"  
b=0.156"

LE #3  
k=0.052"  
b=0.052"

Local conditions at trips?

Sample IR intensity image at t=5 seconds (image 300)

## Test 7071 Run 8



Trip configuration: CL-8; LE-3  
Unit Re: 1.50 Million/ft  
Re-L  
Alpha = 0.0 deg  
Mach = 5.9  
Tunnel set conditions:  
Pt1 = 89.3 psi  
Tt1 = 438.9 °F

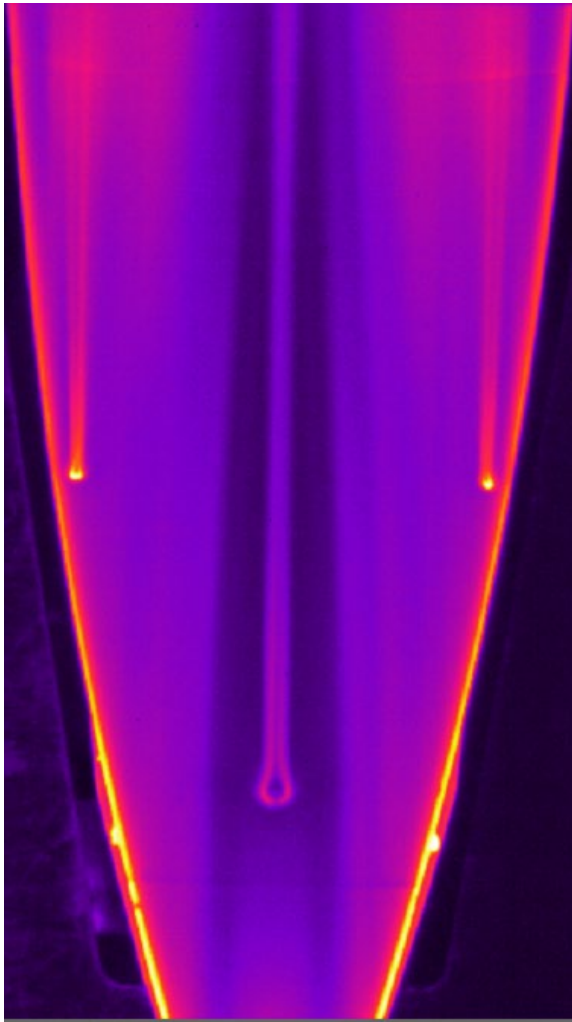
Measured trip dimensions?  
CL #8  
k=0.100"  
b=0.156"

LE #3  
k=0.052"  
b=0.052"

Local conditions at trips?

Sample IR intensity image at t=5 seconds (image 300)

## Test 7071 Run 9



Trip configuration: CL-8; LE-3  
Unit Re: 0.80 Million/ft  
Re-L  
Alpha = 0.0 deg  
Mach = 5.9  
Tunnel set conditions:  
Pt1 = 43.7 psi  
Tt1 = 408.4 °F

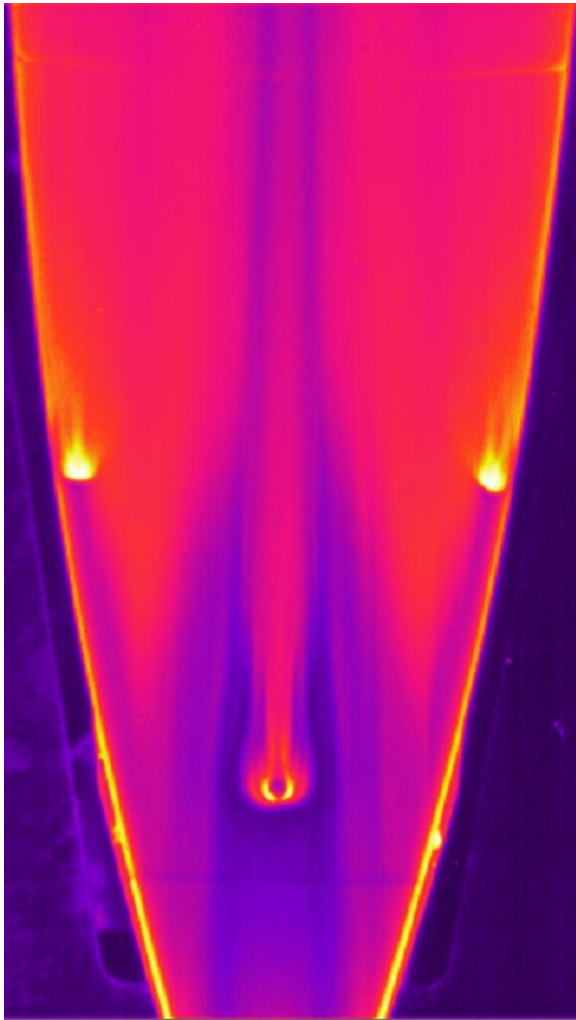
Measured trip dimensions?  
CL #8  
k=0.100"  
b=0.156"

LE #3  
k=0.052"  
b=0.052"

Local conditions at trips?

Sample IR intensity image at t=5 seconds (image 300)

## Test 7071 Run 10



Trip configuration: CL-8; LE-3  
Unit Re: 2.94 Million/ft  
Re-L  
Alpha = 0.0 deg  
Mach = 5.9  
Tunnel set conditions:  
Pt1 = 181.4 psi  
Tt1 = 449.9 °F

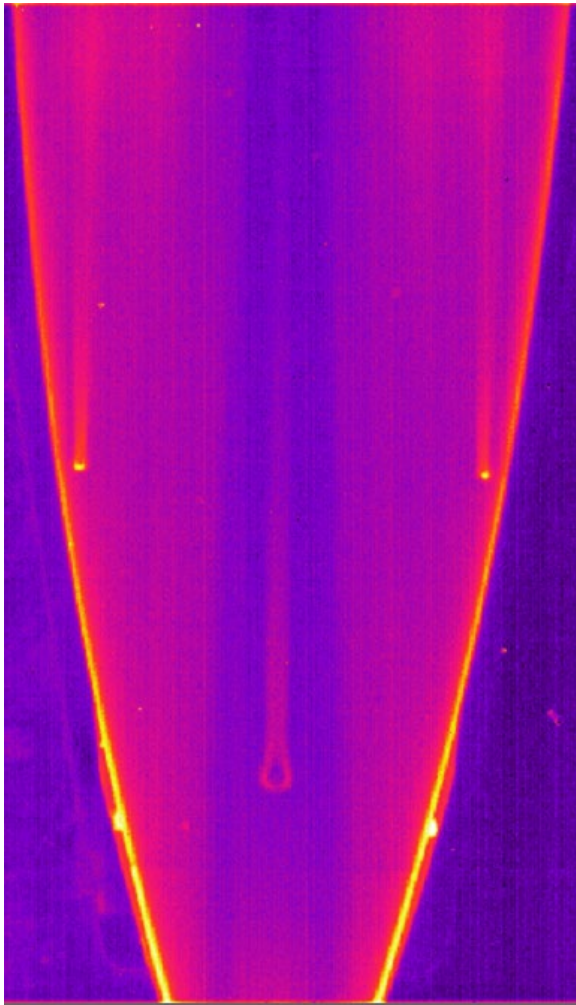
Measured trip dimensions?  
CL #8  
k=0.100"  
b=0.156"  
  
LE #3  
k=0.052"  
b=0.052"

Local conditions at trips?

Sample IR intensity image at t=5 seconds (image 300)



## Test 7071 Run 11



Trip configuration: CL-8; LE-3  
Unit Re: 0.71 Million/ft  
Re-L  
Alpha = 0.0 deg  
Mach = 5.9  
Tunnel set conditions:  
Pt1 = 36.6 psi  
Tt1 = 385.7 °F

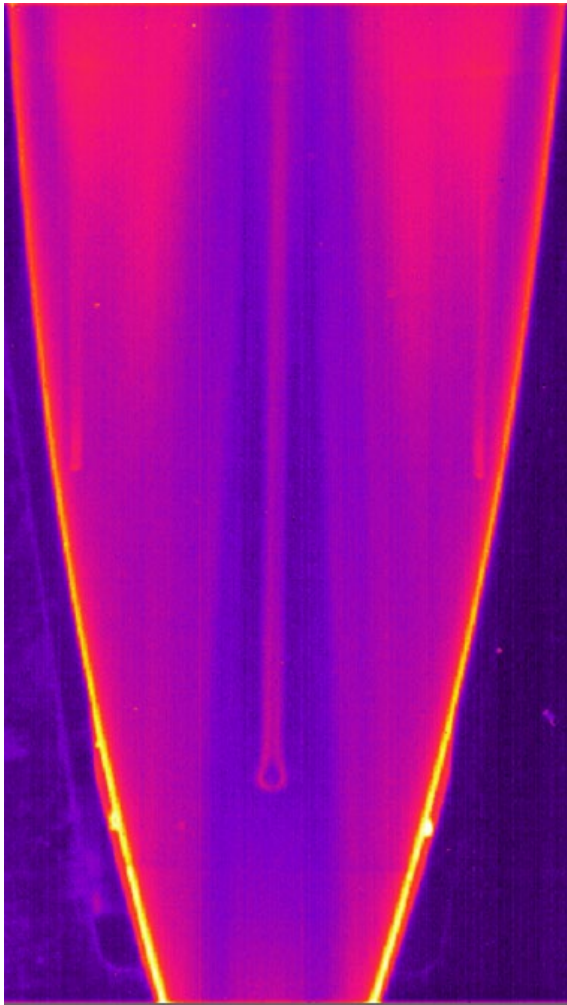
Measured trip dimensions?  
CL #8  
k=0.100"  
b=0.156"

LE #3  
k=0.052"  
b=0.052"

Local conditions at trips?

Sample IR intensity image at t=5 seconds (image 300)

## Test 7071 Run 12



Trip configuration: CL-6; LE-1  
Unit Re: 1.05 Million/ft  
Re-L  
Alpha = 0.0 deg  
Mach = 5.9  
Tunnel set conditions:  
Pt1 = 59.0 psi  
Tt1 = 418.6 °F

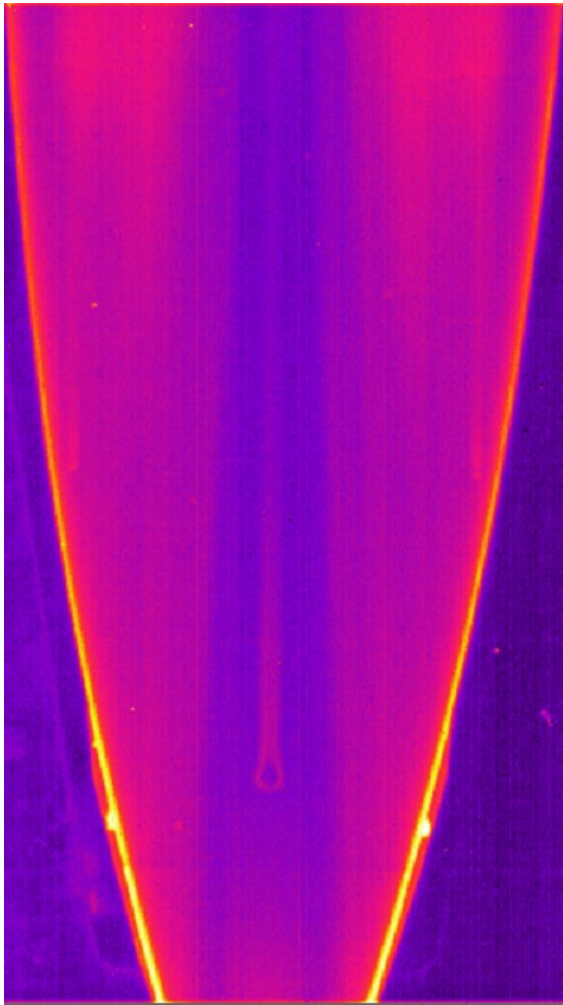
Measured trip dimensions?  
CL #6  
k=0.076"  
b=0.156"

LE #1  
k=0.026"  
b=0.052"

Local conditions at trips?

Sample IR intensity image at t=5 seconds (image 300)

## Test 7071 Run 13



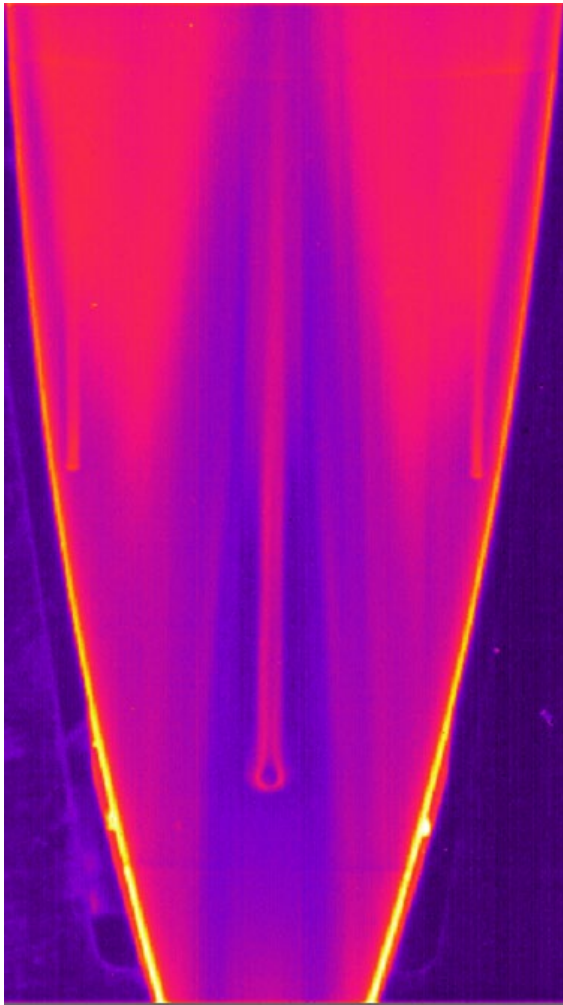
Trip configuration: CL-6; LE-1  
Unit Re: 0.81 Million/ft  
Re-L  
Alpha = 0.0 deg  
Mach = 5.9  
Tunnel set conditions:  
Pt1 = 44.4 psi  
Tt1 = 407.8 °F

Measured trip dimensions?  
CL #6  
k=0.076"  
b=0.156"  
  
LE #1  
k=0.026"  
b=0.052"

Local conditions at trips?

Sample IR intensity image at t=5 seconds (image 300)

## Test 7071 Run 14



Trip configuration: CL-6; LE-1  
Unit Re: 1.51 Million/ft  
Re-L  
Alpha = 0.0 deg  
Mach = 5.9  
Tunnel set conditions:  
Pt1 = 89.4 psi  
Tt1 = 438.3 °F

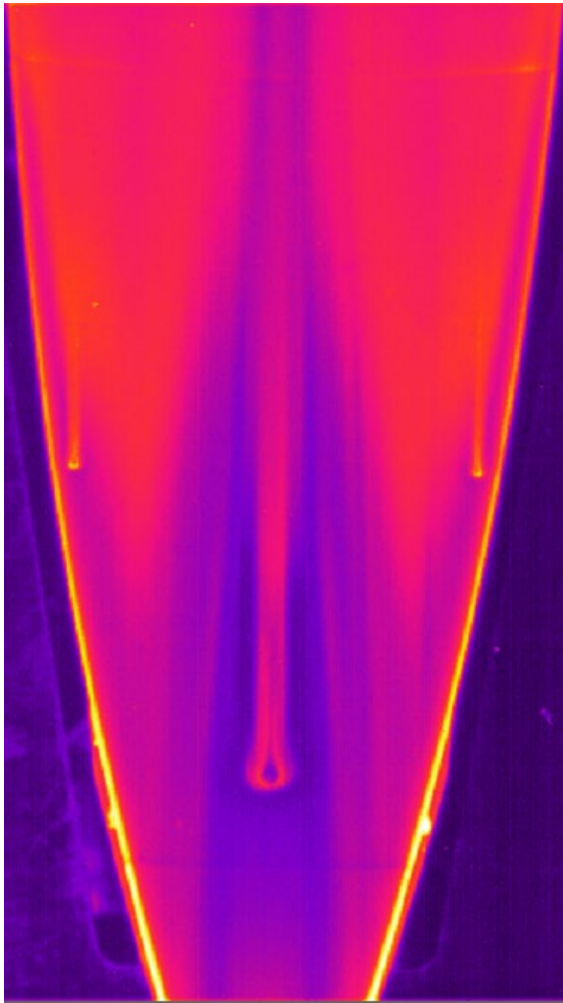
Measured trip dimensions?  
CL #6  
k=0.076"  
b=0.156"

LE #1  
k=0.026"  
b=0.052"

Local conditions at trips?

Sample IR intensity image at t=5 seconds (image 300)

## Test 7071 Run 15



Trip configuration: CL-6; LE-1  
Unit Re: 2.06 Million/ft  
Re-L  
Alpha = 0.0 deg  
Mach = 5.9  
Tunnel set conditions:  
Pt1 = 125.8 psi  
Tt1 = 448.5 °F

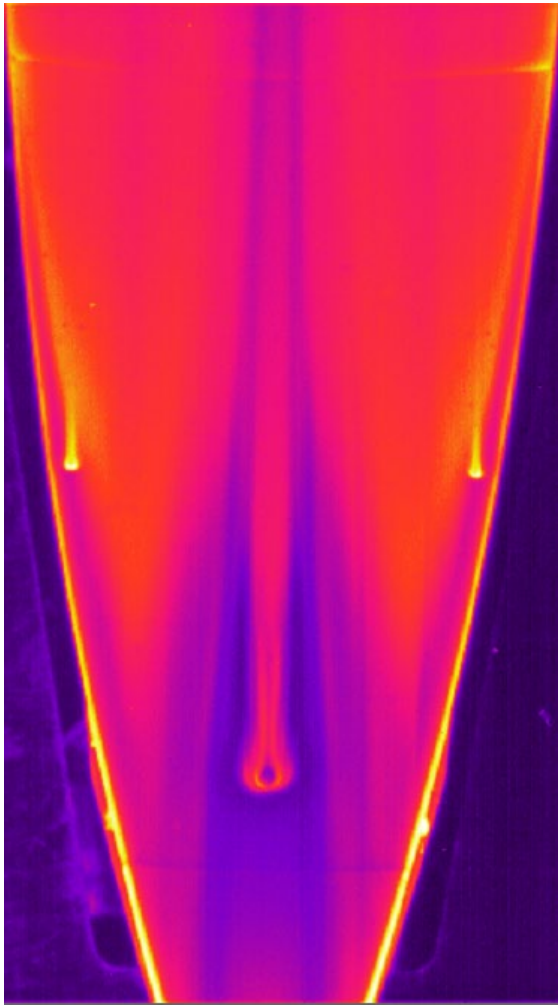
Measured trip dimensions?  
CL #6  
k=0.076"  
b=0.156"

LE #1  
k=0.026"  
b=0.052"

Local conditions at trips?

Sample IR intensity image at t=5 seconds (image 300)

## Test 7071 Run 16



Trip configuration: CL-6; LE-1  
Unit Re: 2.98 Million/ft  
Re-L  
Alpha = 0.0 deg  
Mach = 5.9  
Tunnel set conditions:  
Pt1 = 183.8 psi  
Tt1 = 448.1 °F

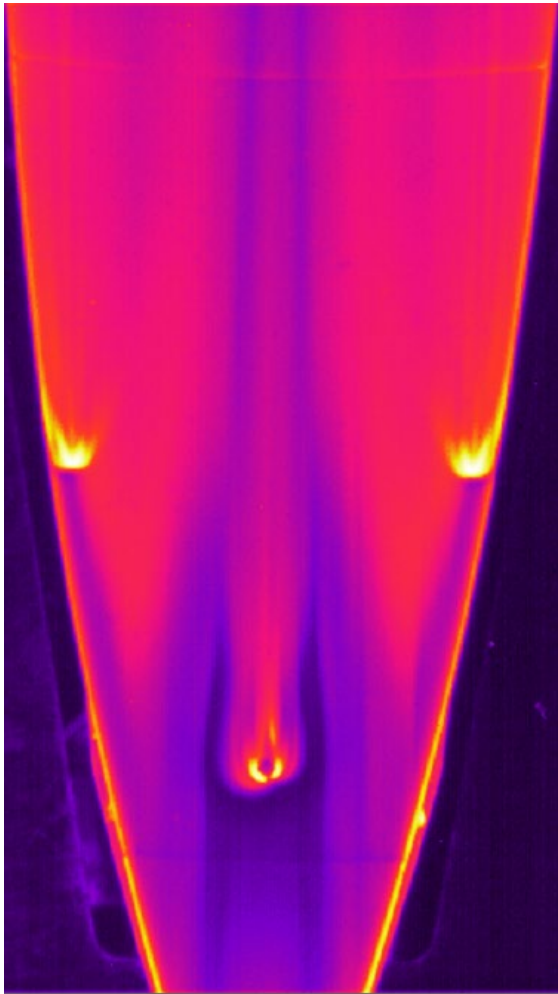
Measured trip dimensions?  
CL #6  
k=0.076"  
b=0.156"

LE #1  
k=0.026"  
b=0.052"

Local conditions at trips?

Sample IR intensity image at t=5 seconds (image 300)

## Test 7071 Run 17



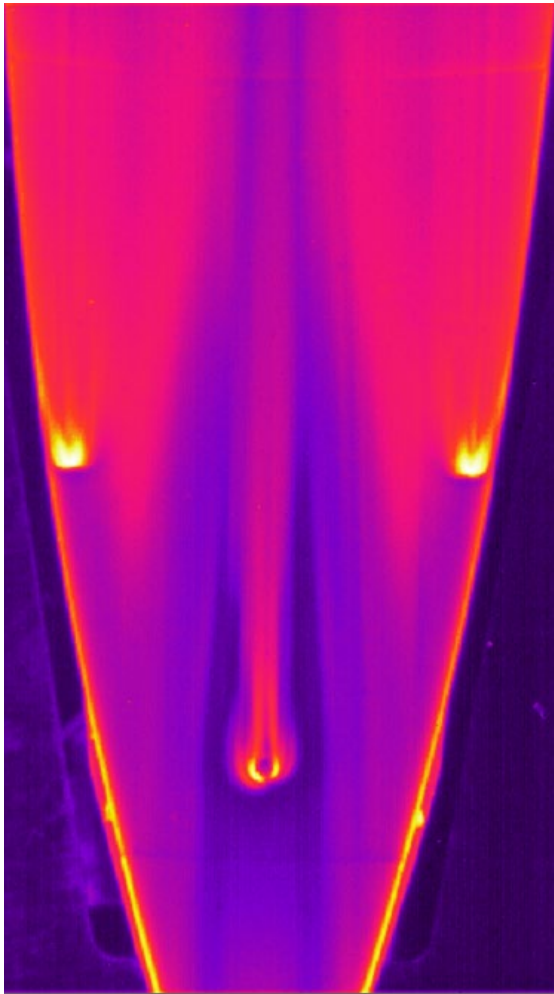
Trip configuration: CL-10; LE-5  
Unit Re: 2.97 Million/ft  
Re-L  
Alpha = 0.0 deg  
Mach = 5.9  
Tunnel set conditions:  
Pt1 = 182.9 psi  
Tt1 = 449.0 °F

Measured trip dimensions?  
CL #10  
k=0.124"  
b=0.156"  
  
LE #5  
k=0.076"  
b=0.052"

Local conditions at trips?

Sample IR intensity image at t=5 seconds (image 300)

## Test 7071 Run 18



Trip configuration: CL-10; LE-5  
Unit Re: 2.05 Million/ft  
Re-L  
Alpha = 0.0 deg  
Mach = 5.9  
Tunnel set conditions:  
Pt1 = 125.0 psi  
Tt1 = 447.2 °F

Measured trip dimensions?  
CL #10  
k=0.124"  
b=0.156"

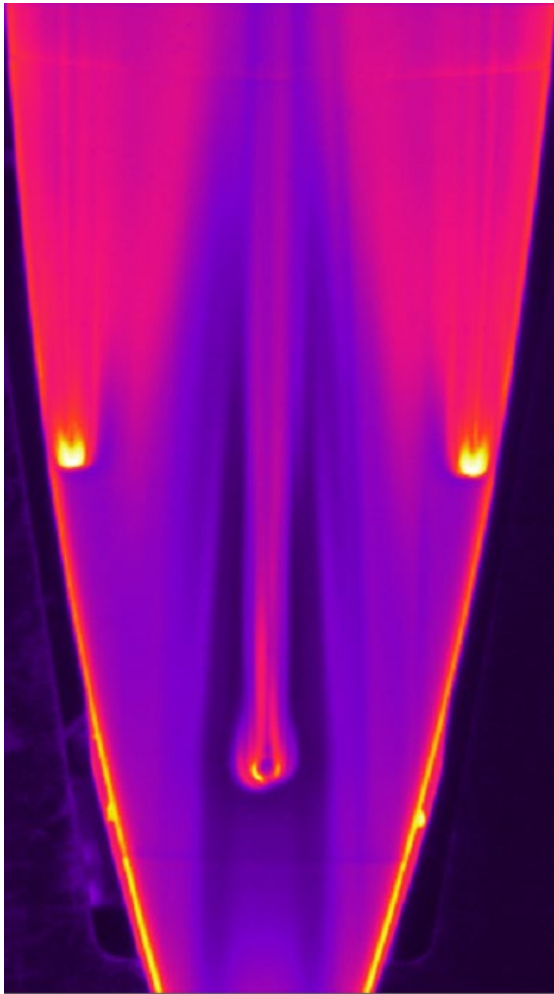
LE #5  
k=0.076"  
b=0.052"

Local conditions at trips?

Sample IR intensity image at t=5 seconds (image 300)



## Test 7071 Run 19



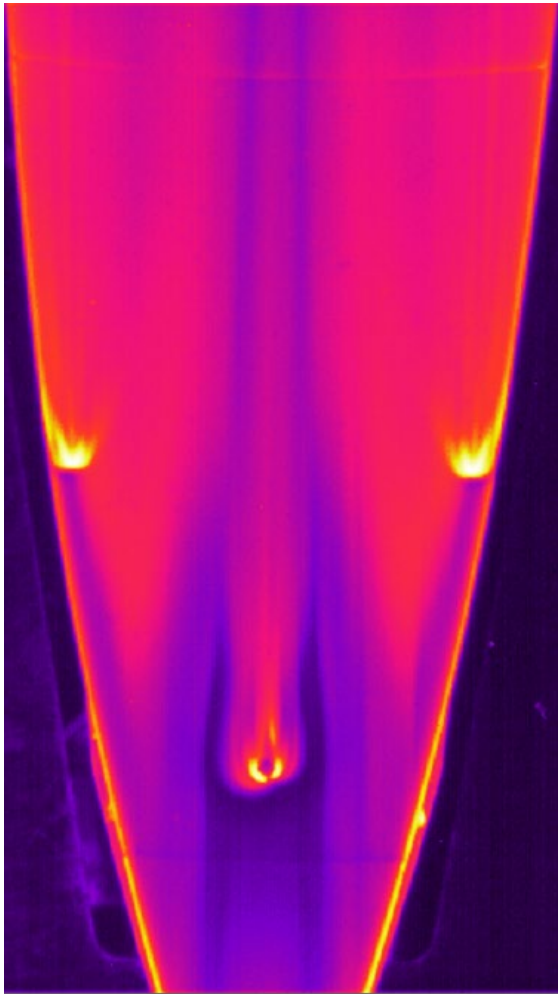
Trip configuration: CL-10; LE-5  
Unit Re: 1.51 Million/ft  
Re-L  
Alpha = 0.0 deg  
Mach = 5.9  
Tunnel set conditions:  
Pt1 = 89.8 psi  
Tt1 = 438.0 °F

Measured trip dimensions?  
CL #10  
k=0.124"  
b=0.156"  
  
LE #5  
k=0.076"  
b=0.052"

Local conditions at trips?

Sample IR intensity image at t=5 seconds (image 300)

## Test 7071 Run 20



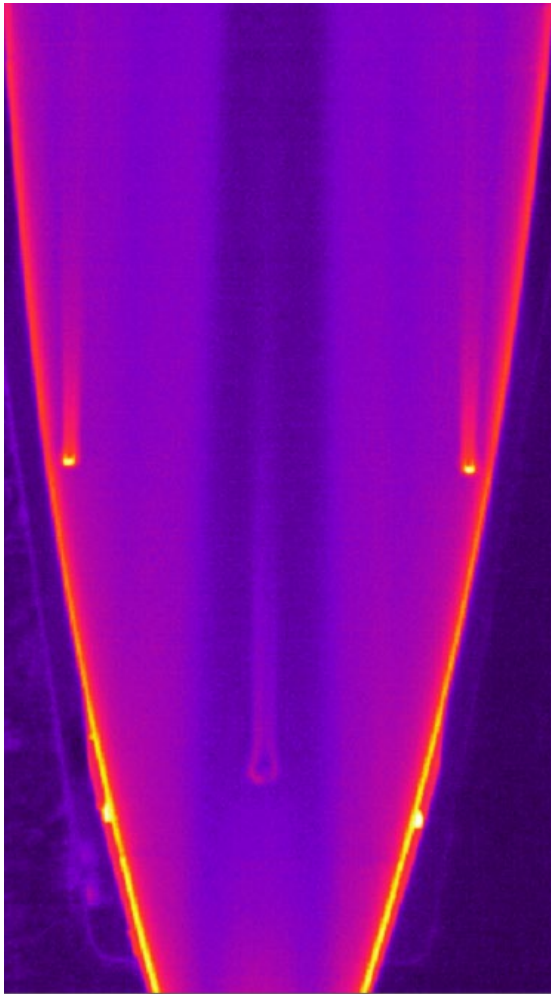
Trip configuration: CL-10; LE-5  
Unit Re: 1.06 Million/ft  
Re-L  
Alpha = 0.0 deg  
Mach = 5.9  
Tunnel set conditions:  
Pt1 = 59.7 psi  
Tt1 = 417.6 °F

Measured trip dimensions?  
CL #10  
k=0.124"  
b=0.156"  
  
LE #5  
k=0.076"  
b=0.052"

Local conditions at trips?

Sample IR intensity image at t=5 seconds (image 300)

## Test 7071 Run 21



Trip configuration: CL-10; LE-5  
Unit Re: 0.38 Million/ft  
Re-L  
Alpha = 0.0 deg  
Mach = 5.9  
Tunnel set conditions:  
Pt1 = 17.5 psi  
Tt1 = 345.2 °F

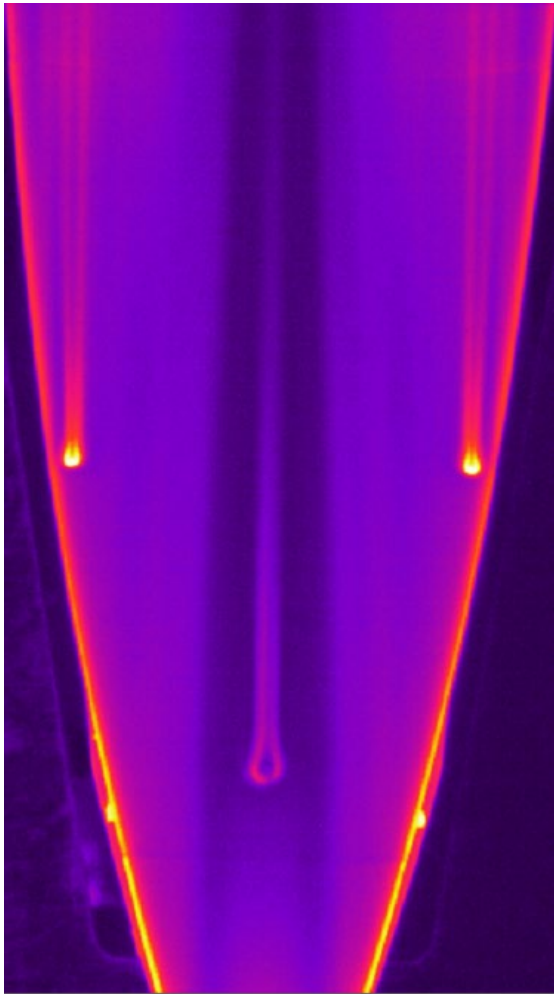
Measured trip dimensions?  
CL #10  
k=0.124"  
b=0.156"

LE #5  
k=0.076"  
b=0.052"

Local conditions at trips?

Sample IR intensity image at t=5 seconds (image 300)

## Test 7071 Run 22



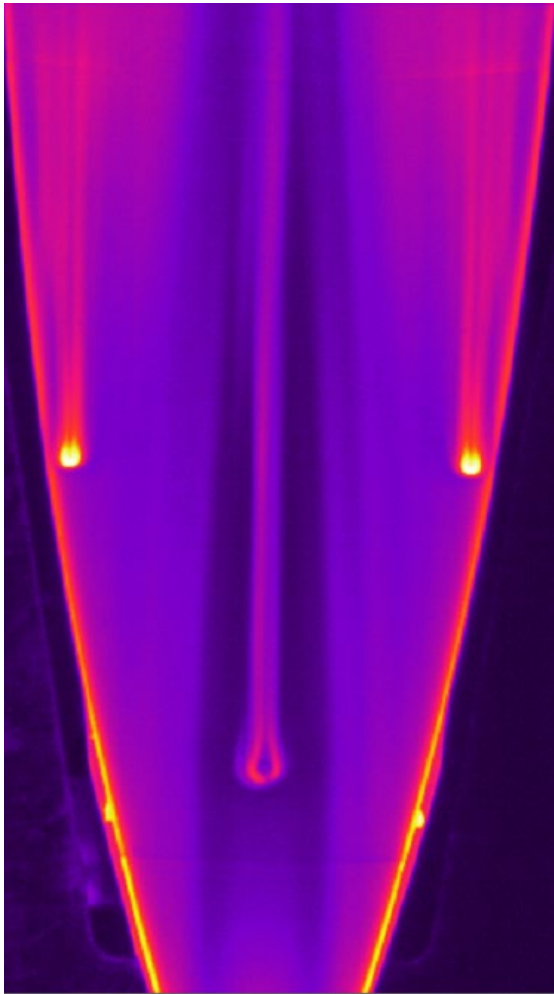
Trip configuration: CL-10; LE-5  
Unit Re: 0.58 Million/ft  
Re-L  
Alpha = 0.0 deg  
Mach = 5.9  
Tunnel set conditions:  
Pt1 = 29.5 psi  
Tt1 = 386.0 °F

Measured trip dimensions?  
CL #10  
k=0.124"  
b=0.156"  
  
LE #5  
k=0.076"  
b=0.052"

Local conditions at trips?

Sample IR intensity image at t=5 seconds (image 300)

## Test 7071 Run 23



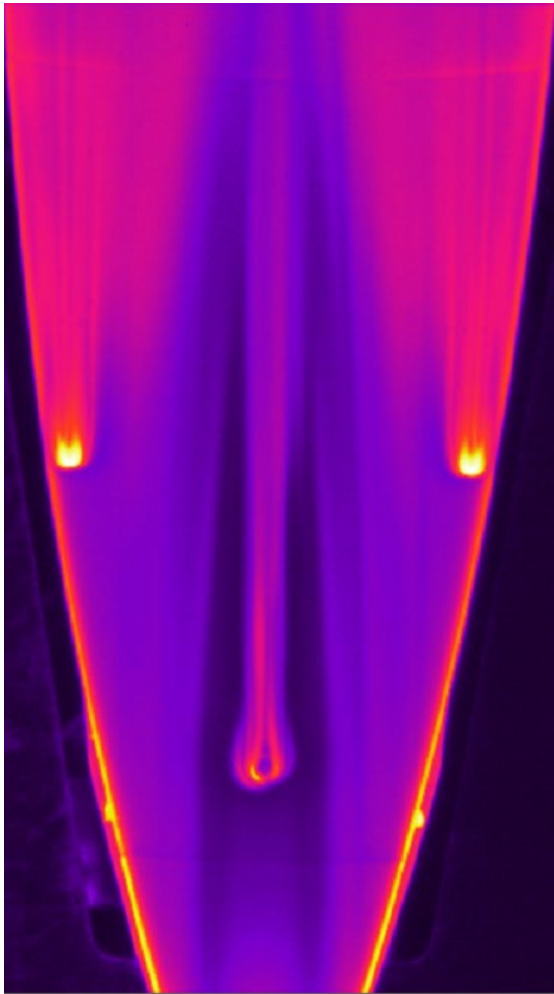
Trip configuration: CL-10; LE-5  
Unit Re: 0.82 Million/ft  
Re-L  
Alpha = 0.0 deg  
Mach = 5.9  
Tunnel set conditions:  
Pt1 = 44.9 psi  
Tt1 = 408.1 °F

Measured trip dimensions?  
CL #10  
k=0.124"  
b=0.156"  
  
LE #5  
k=0.076"  
b=0.052"

Local conditions at trips?

Sample IR intensity image at t=5 seconds (image 300)

## Test 7071 Run 24



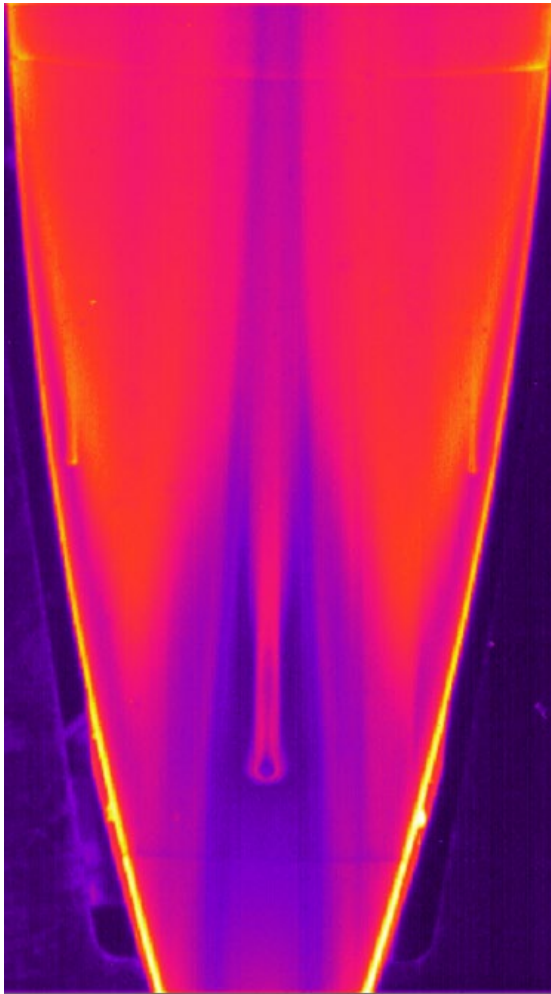
Trip configuration: CL-10; LE-5  
Unit Re: 1.26 Million/ft  
Re-L  
Alpha = 0.0 deg  
Mach = 5.9  
Tunnel set conditions:  
Pt1 = 73.7 psi  
Tt1 = 435.0 °F

Measured trip dimensions?  
CL #10  
k=0.124"  
b=0.156"  
  
LE #5  
k=0.076"  
b=0.052"

Local conditions at trips?

Sample IR intensity image at t=5 seconds (image 300)

## Test 7071 Run 25



Trip configuration: CL-4; LE-11  
Unit Re: 2.96 Million/ft  
Re-L  
Alpha = 0.0 deg  
Mach = 5.9  
Tunnel set conditions:  
Pt1 = 182.3 psi  
Tt1 = 448.7 °F

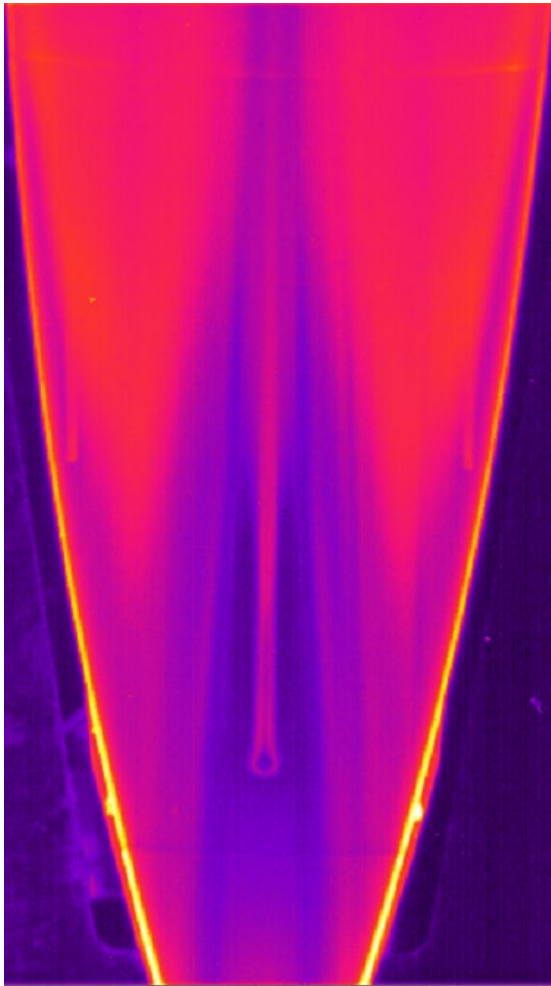
Measured trip dimensions?  
CL #4  
k=0.052"  
b=0.156"

LE #5  
k=0.018"  
b=0.052"

Local conditions at trips?

Sample IR intensity image at t=5 seconds (image 300)

## Test 7071 Run 26



Trip configuration: CL-4; LE-11  
Unit Re: 2.04 Million/ft  
Re-L  
Alpha = 0.0 deg  
Mach = 5.9  
Tunnel set conditions:  
Pt1 = 124.6 psi  
Tt1 = 448.2 °F

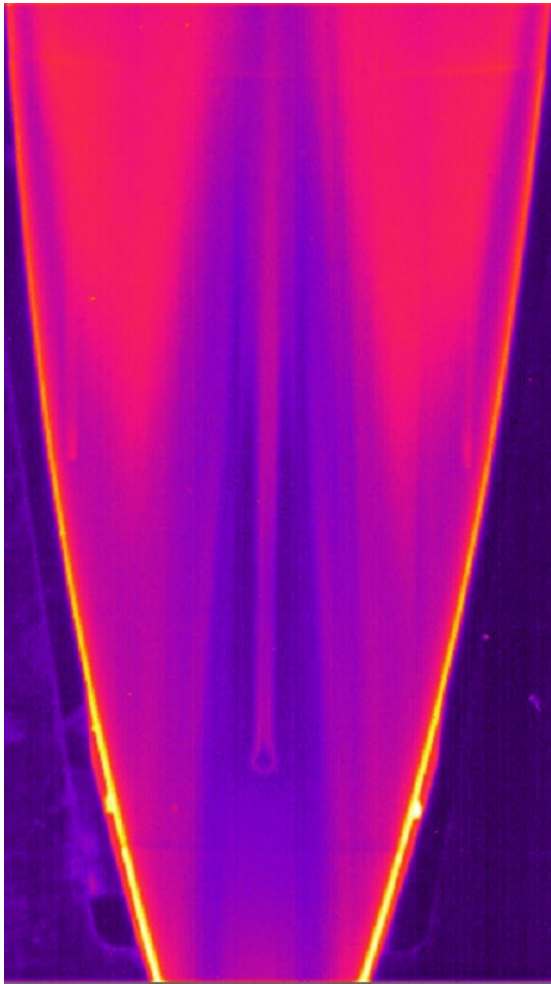
Measured trip dimensions?  
CL #4  
k=0.052"  
b=0.156"  
  
LE #5  
k=0.018"  
b=0.052"

Local conditions at trips?

Sample IR intensity image at t=5 seconds (image 300)



## Test 7071 Run 27



Trip configuration: CL-4; LE-11  
Unit Re: 1.50 Million/ft  
Re-L  
Alpha = 0.0 deg  
Mach = 5.9  
Tunnel set conditions:  
Pt1 = 89.0 psi  
Tt1 = 439.0 °F

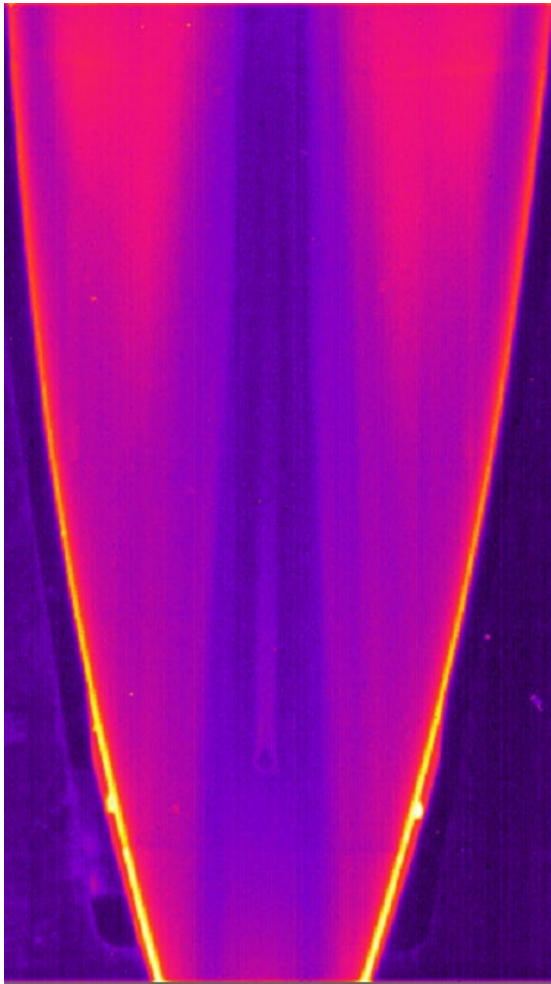
Measured trip dimensions?  
CL #4  
k=0.052"  
b=0.156"

LE #5  
k=0.018"  
b=0.052"

Local conditions at trips?

Sample IR intensity image at t=5 seconds (image 300)

## Test 7071 Run 28



Trip configuration: CL-4; LE-11  
Unit Re: 1.12 Million/ft  
Re-L  
Alpha = 0.0 deg  
Mach = 5.9  
Tunnel set conditions:  
Pt1 = 64.1 psi  
Tt1 = 424.0 °F

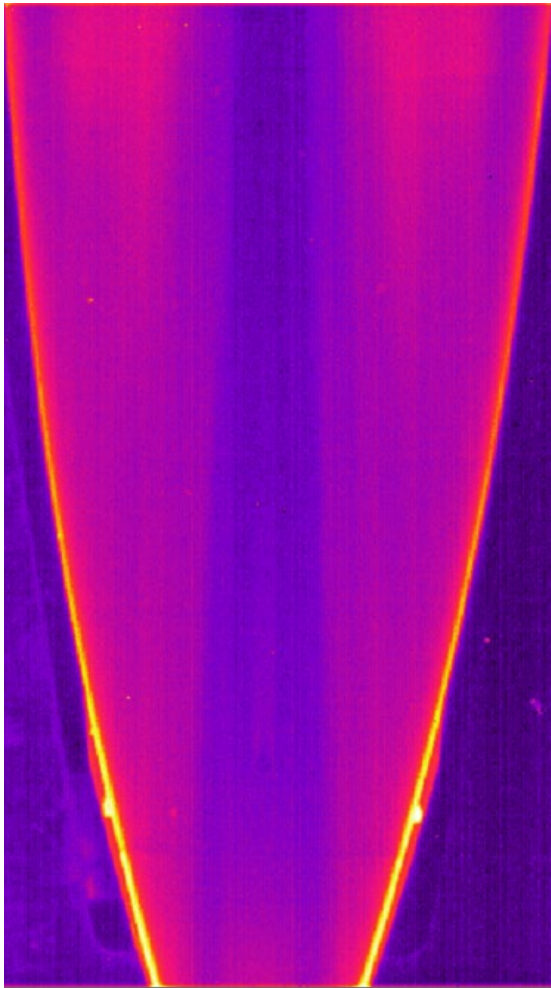
Measured trip dimensions?  
CL #4  
k=0.052"  
b=0.156"

LE #5  
k=0.018"  
b=0.052"

Local conditions at trips?

Sample IR intensity image at t=5 seconds (image 300)

## Test 7071 Run 29



Trip configuration: CL-4; LE-11  
Unit Re: 0.81 Million/ft  
Re-L  
Alpha = 0.0 deg  
Mach = 5.9  
Tunnel set conditions:  
Pt1 = 44.4 psi  
Tt1 = 407.5 °F

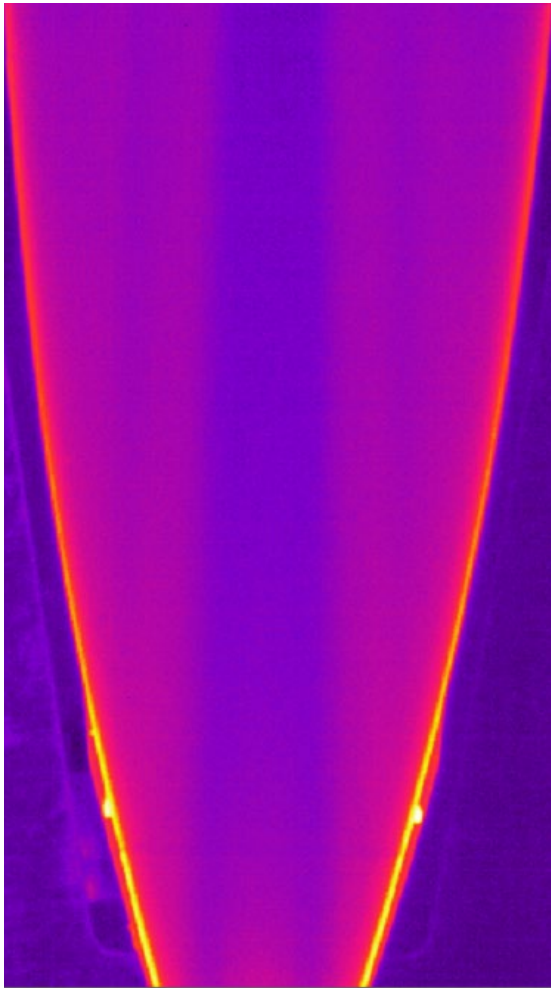
Measured trip dimensions?  
CL #4  
k=0.052"  
b=0.156"

LE #5  
k=0.018"  
b=0.052"

Local conditions at trips?

Sample IR intensity image at t=5 seconds (image 300)

## Test 7071 Run 30



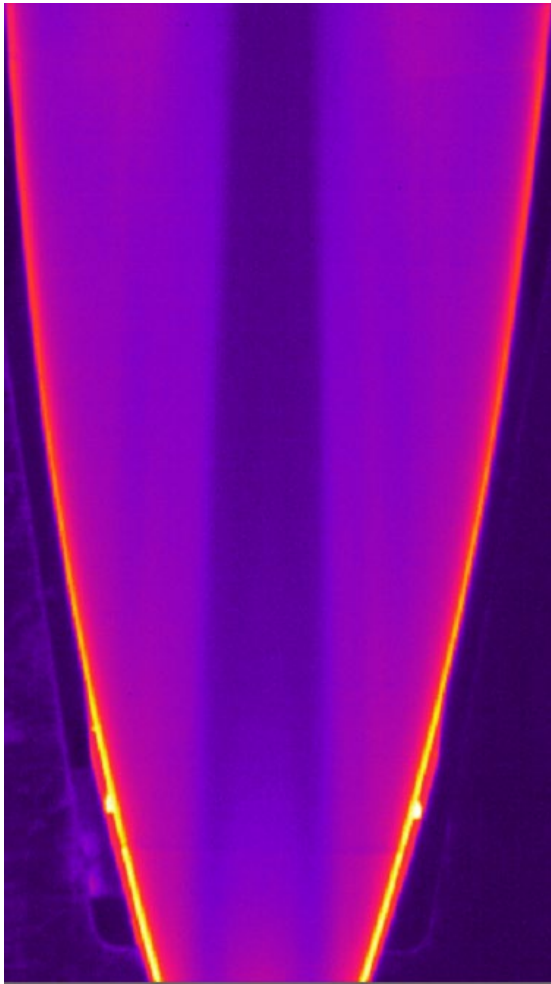
No Trip Baseline  
Unit Re: 0.34 Million/ft  
Re-L  
Alpha = 0.0 deg  
Mach = 5.9  
Tunnel set conditions:  
Pt1 = 15.7 psi  
Tt1 = 356.7 °F

No Trip Baseline

Local conditions at trips?

Sample IR intensity image at t=5 seconds (image 300)

## Test 7071 Run 31



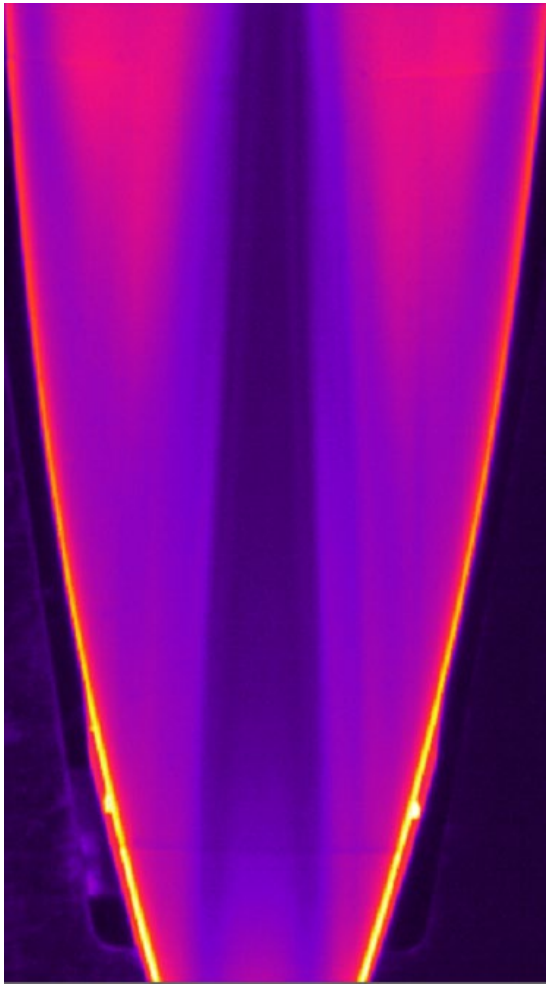
No Trip Baseline  
Unit Re: 0.57 Million/ft  
Re-L  
Alpha = 0.0 deg  
Mach = 5.9  
Tunnel set conditions:  
Pt1 = 29.7 psi  
Tt1 = 400.6 °F

No Trip Baseline

Local conditions at trips?

Sample IR intensity image at t=5 seconds (image 300)

## Test 7071 Run 32



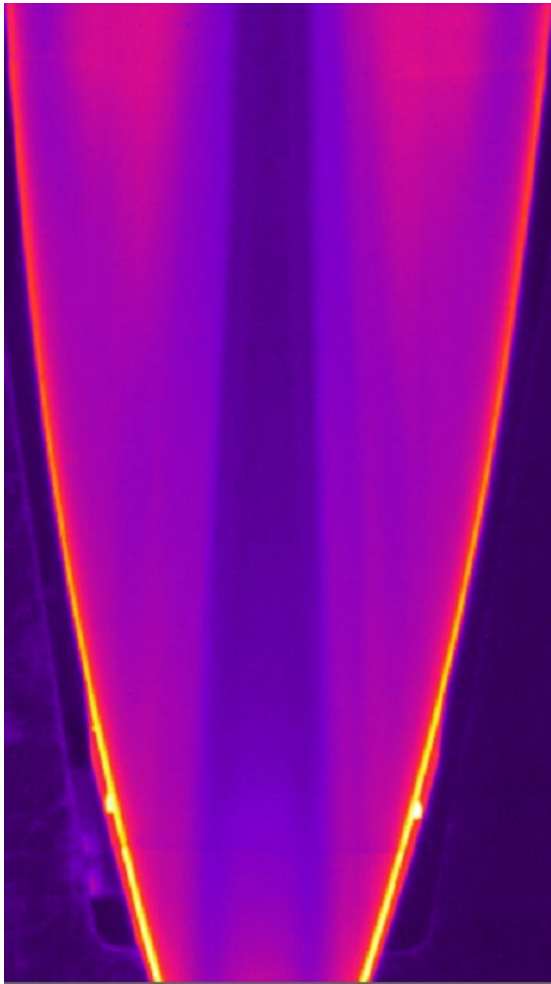
No Trip Baseline  
Unit Re: 1.05 Million/ft  
Re-L  
Alpha = 0.0 deg  
Mach = 5.9  
Tunnel set conditions:  
Pt1 = 59.7 psi  
Tt1 = 421.1 °F

No Trip Baseline

Local conditions at trips?

Sample IR intensity image at t=5 seconds (image 300)

## Test 7071 Run 33



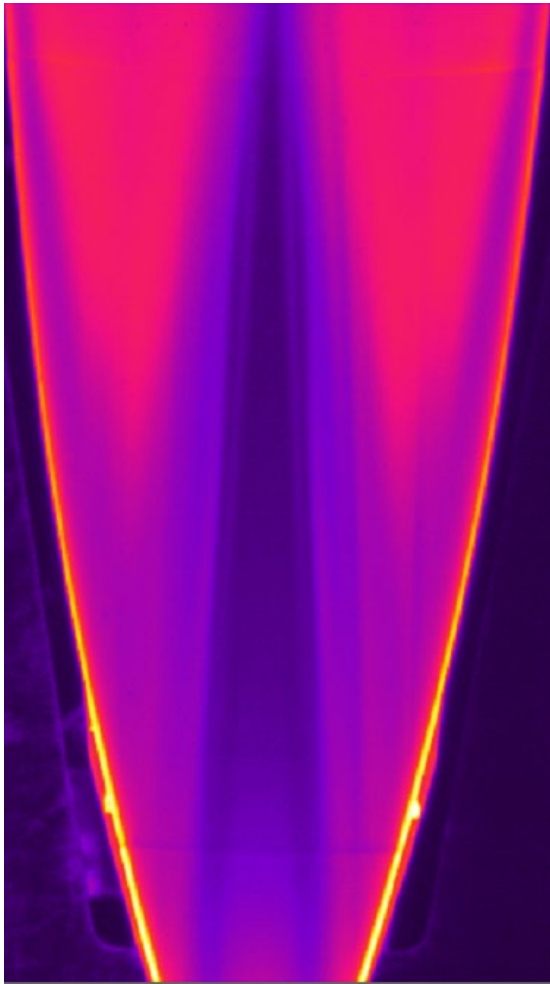
No Trip Baseline  
Unit Re: 0.82 Million/ft  
Re-L  
Alpha = 0.0 deg  
Mach = 5.9  
Tunnel set conditions:  
Pt1 = 45.0 psi  
Tt1 = 408.4 °F

No Trip Baseline

Local conditions at trips?

Sample IR intensity image at t=5 seconds (image 300)

## Test 7071 Run 34



No Trip Baseline  
Unit Re: 1.52 Million/ft  
Re-L  
Alpha = 0.0 deg  
Mach = 5.9  
Tunnel set conditions:  
Pt1 = 90.1 psi  
Tt1 = 438.8 °F

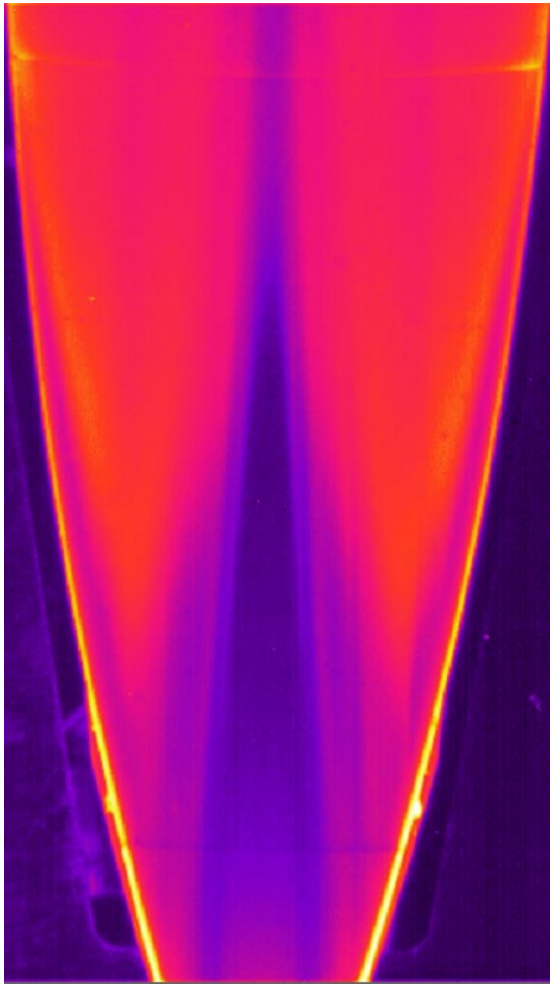
No Trip Baseline

Local conditions at trips?

Sample IR intensity image at t=5 seconds (image 300)



## Test 7071 Run 35



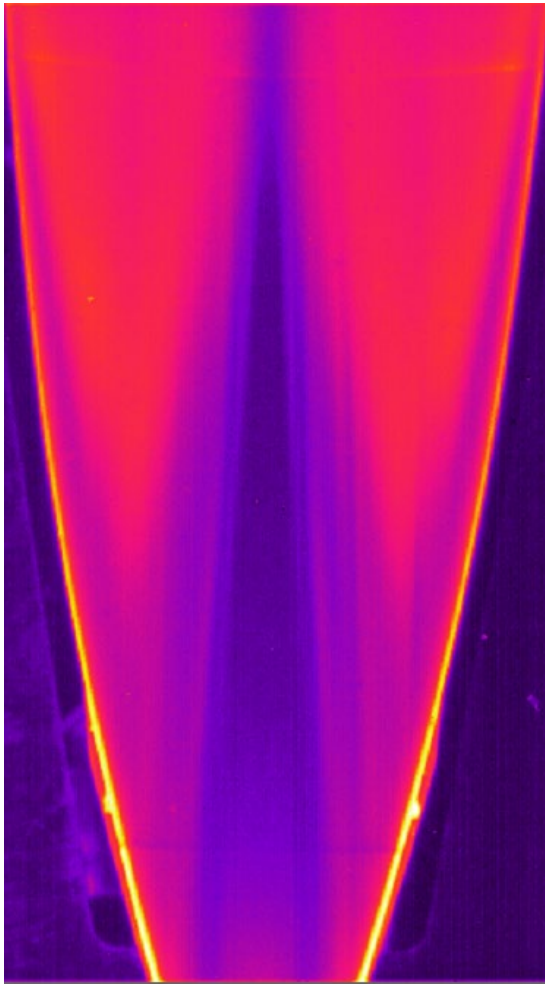
No Trip Baseline  
Unit Re: 2.95 Million/ft  
Re-L  
Alpha = 0.0 deg  
Mach = 5.9  
Tunnel set conditions:  
Pt1 = 182.1 psi  
Tt1 = 448.6 °F

No Trip Baseline

Local conditions at trips?

Sample IR intensity image at t=5 seconds (image 300)

## Test 7071 Run 36



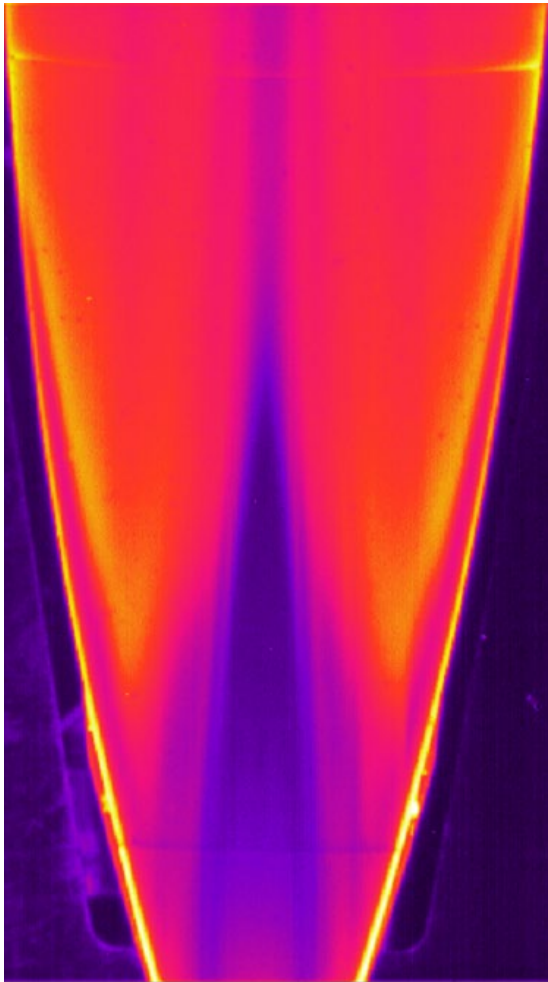
No Trip Baseline  
Unit Re: 2.03 Million/ft  
Re-L  
Alpha = 0.0 deg  
Mach = 5.9  
Tunnel set conditions:  
Pt1 = 124.1 psi  
Tt1 = 447.6 °F

No Trip Baseline

Local conditions at trips?

Sample IR intensity image at t=5 seconds (image 300)

## Test 7071 Run 37



No Trip Baseline  
Unit Re: 4.07 Million/ft  
Re-L  
Alpha = 0.0 deg  
Mach = 5.9  
Tunnel set conditions:  
Pt1 = 253.2 psi  
Tt1 = 450.9 °F

No Trip Baseline

Local conditions at trips?

Sample IR intensity image at t=5 seconds  
(image 300)

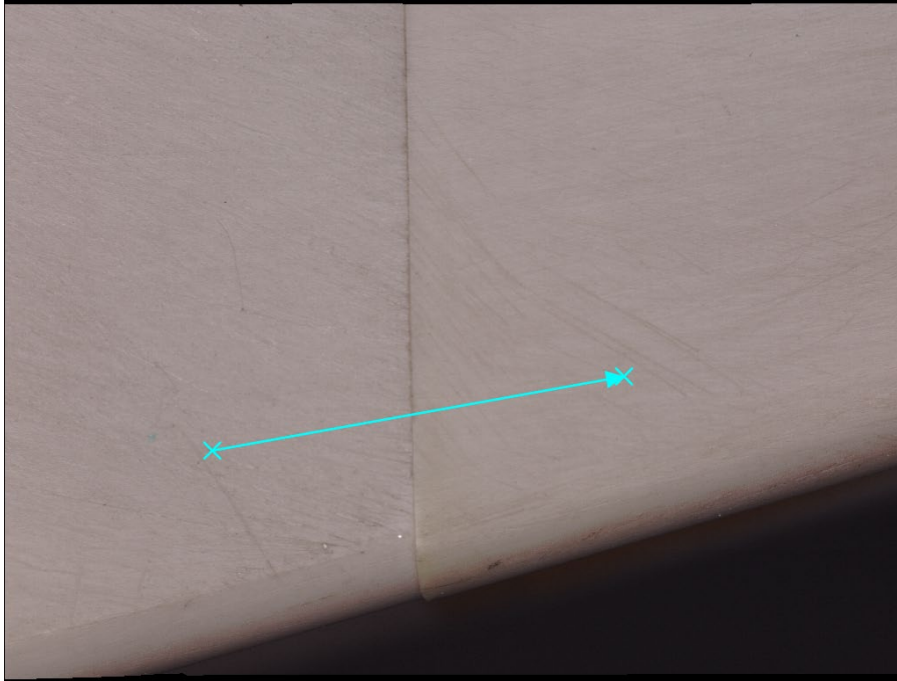
## Appendix B

A digital microscope was used to obtain high resolution images of the assembled model with key parts attached, as contained in the subsequent pages of this appendix. Measurements were made with a Keyence VR-3200, Wide-Area 3D Measurement System. These magnified images were used to measure both the heights above the surface of each location of interest and any lateral dimensions required. The stated accuracy of these measurements based on the manufacturer's literature is  $\pm 3\mu\text{m}$  (or 0.00012") in vertical height and  $\pm 2\text{-}5\mu\text{m}$  (or 0.000079-0.00020") in horizontal width (depending on level of magnification).

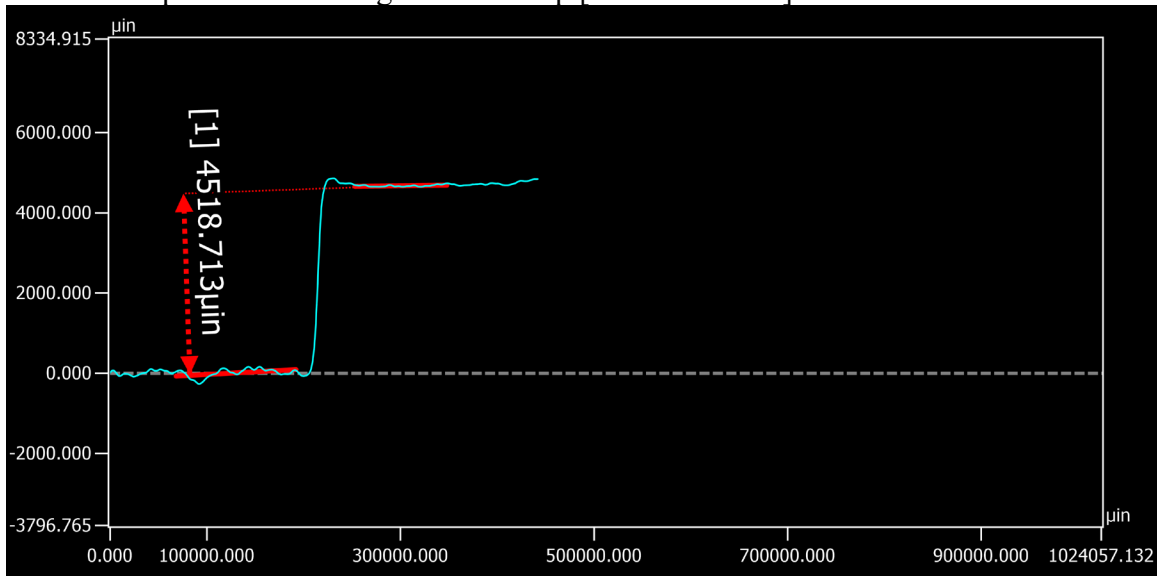
The following pages of this appendix provide the detailed measurements of the model nose-joint step with the only insert used during this test entry (-03b, installed at the beginning of test and never changed until measured), as well as all the trips (#1-11) temporarily installed (posttest) in the CL trip location.

**Scans of the nose-joint step with insert -3b installed**

Right side of nose step:



Location of profile data on right side of step [Source: NASA].

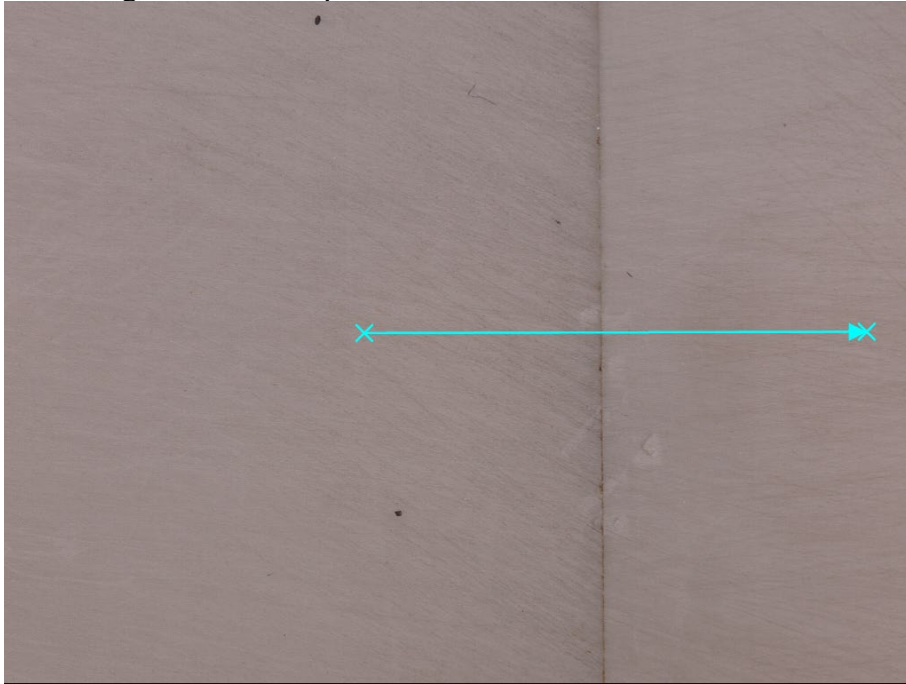


Profile data from line shown above.

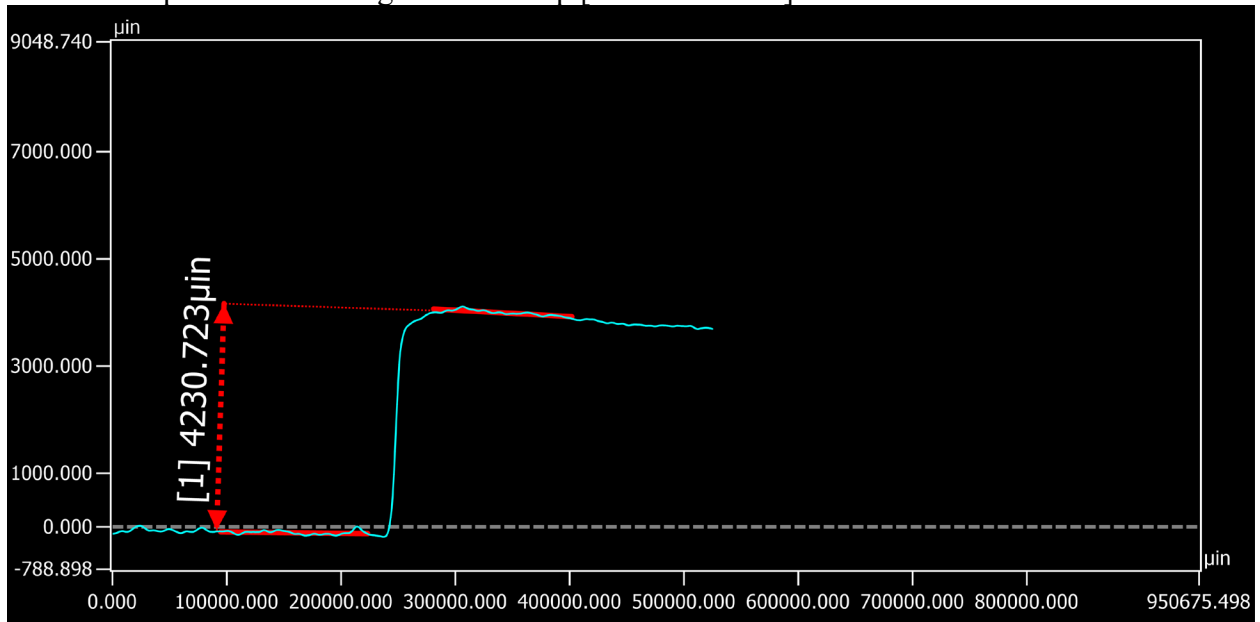
Rearward facing (RF) step of 0.0045” on right side of model.

Appendix B - Digital Microscope Results

Center region of nose step:



Location of profile data on right side of step [Source: NASA].

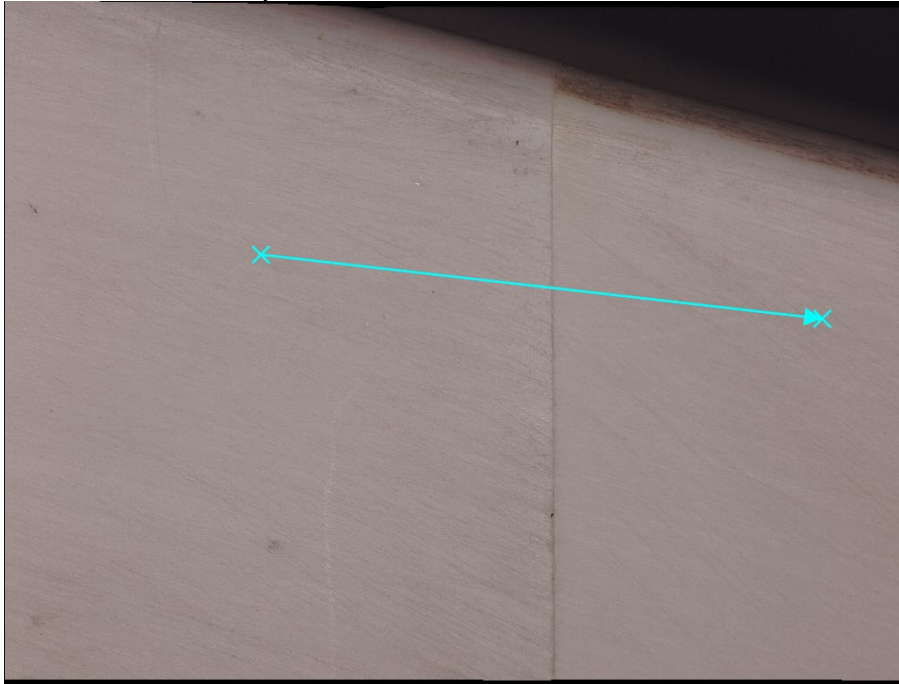


Profile data from line shown above.

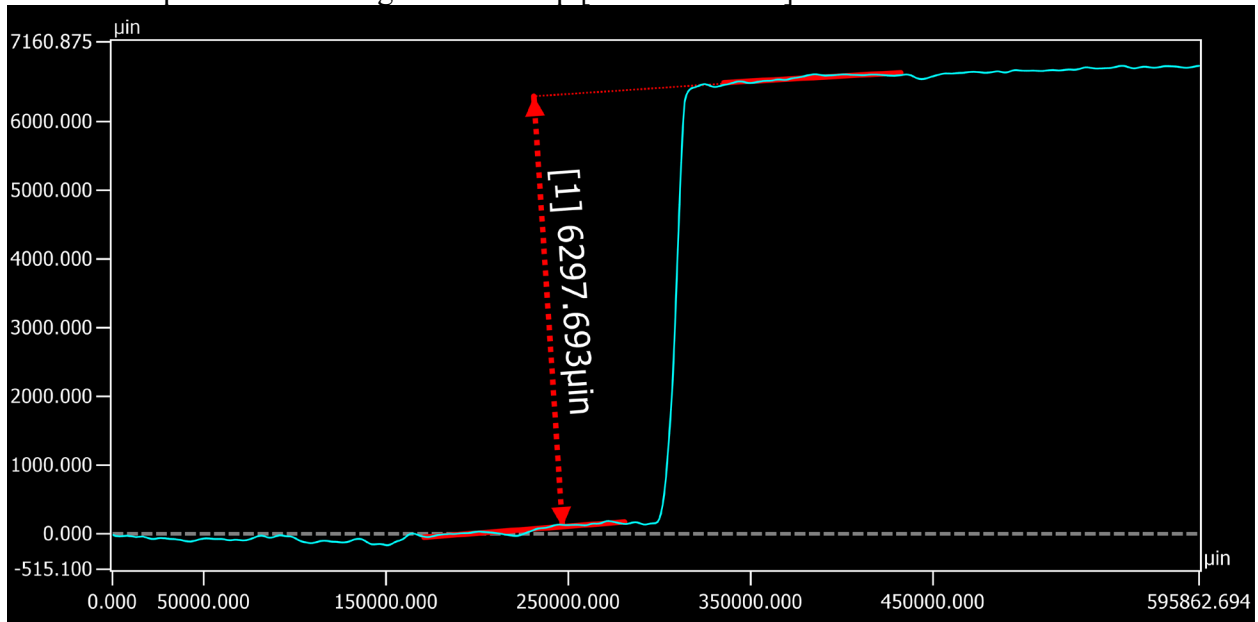
Rearward facing (RF) step of 0.0042” on the center region of model.

## Appendix B - Digital Microscope Results

Left side of nose step:



Location of profile data on right side of step [Source: NASA].



Profile data from line shown above.

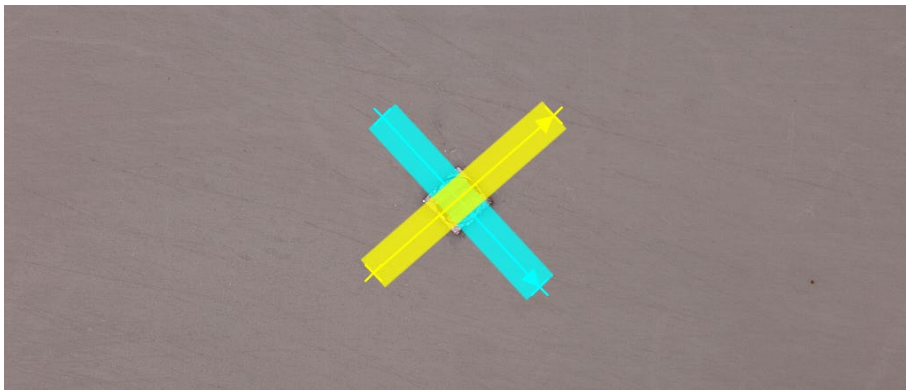
Rearward facing (RF) step of 0.0063" on left side of model.

Appendix B - Digital Microscope Results

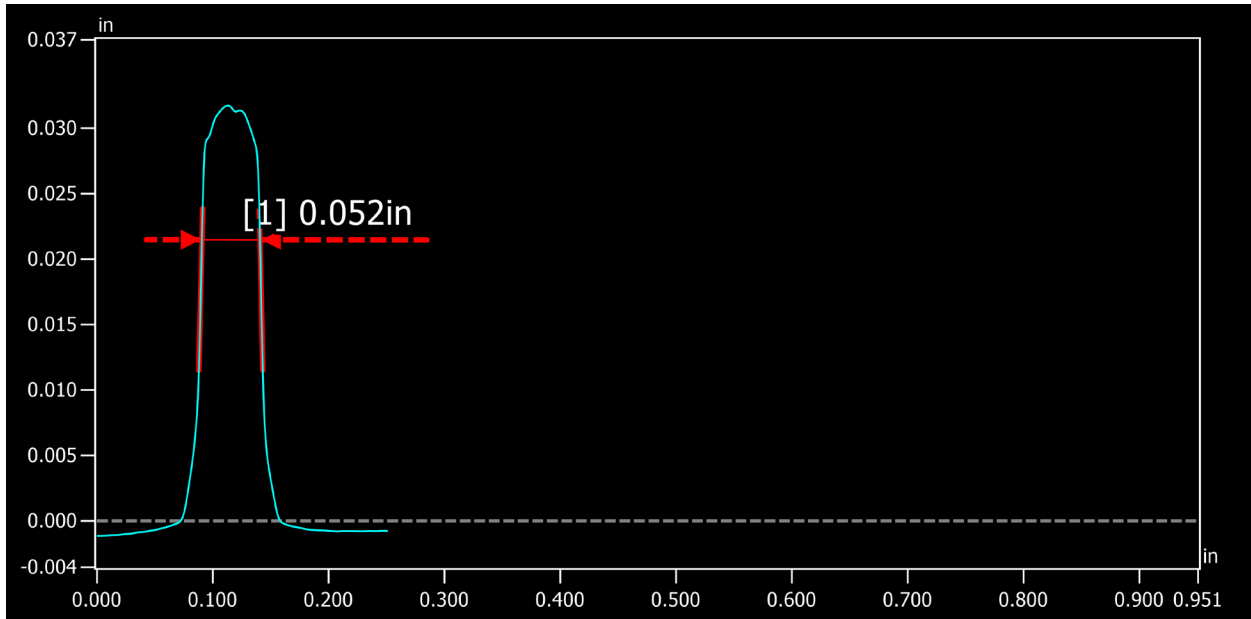
**Trip #1 (notionally  $k=0.026''$ ,  $b=0.052''$ )**



12x Optical image [Source: NASA].



Profile locations shown (20 averages for each) [Source: NASA].

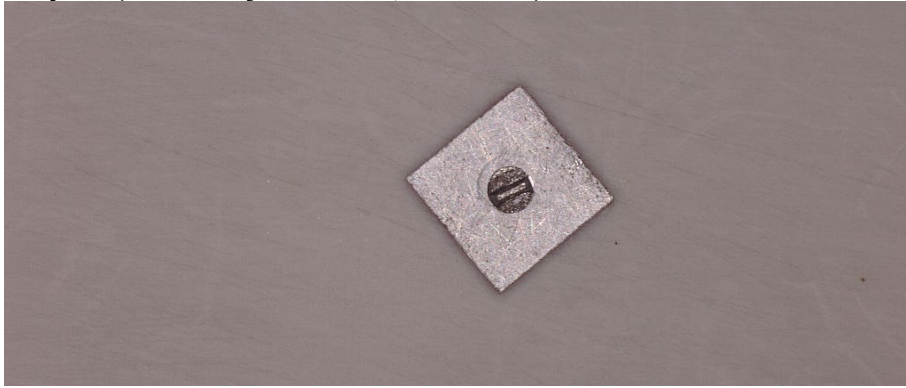


Measured  $k=0.031''$  and  $b=0.052''$

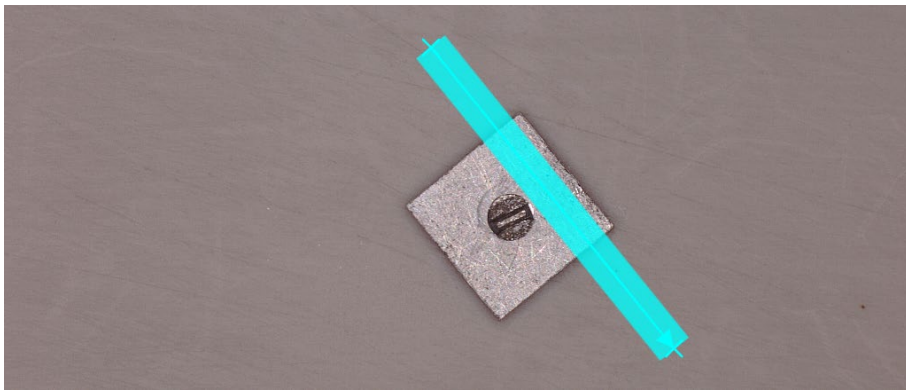


Appendix B - Digital Microscope Results

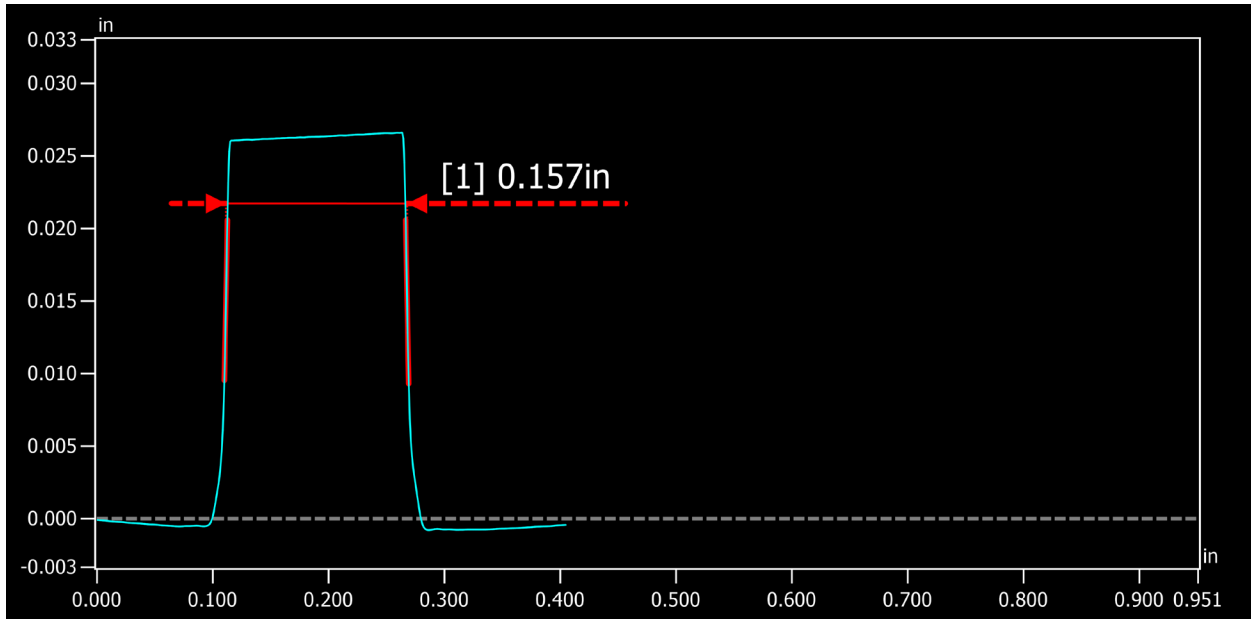
Trip #2 (notionally  $k=0.026''$ ,  $b=0.156''$ )



12x Optical image [Source: NASA].



Profile locations shown (20 averages) [Source: NASA].



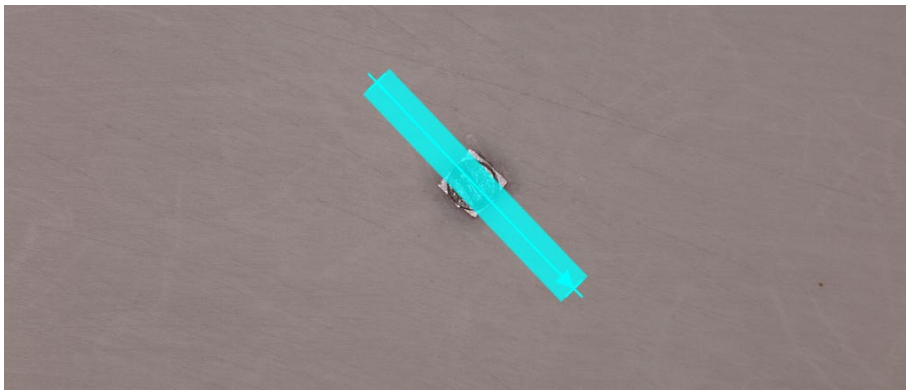
Measured  $k=0.026''$  and  $b=0.157''$

Appendix B - Digital Microscope Results

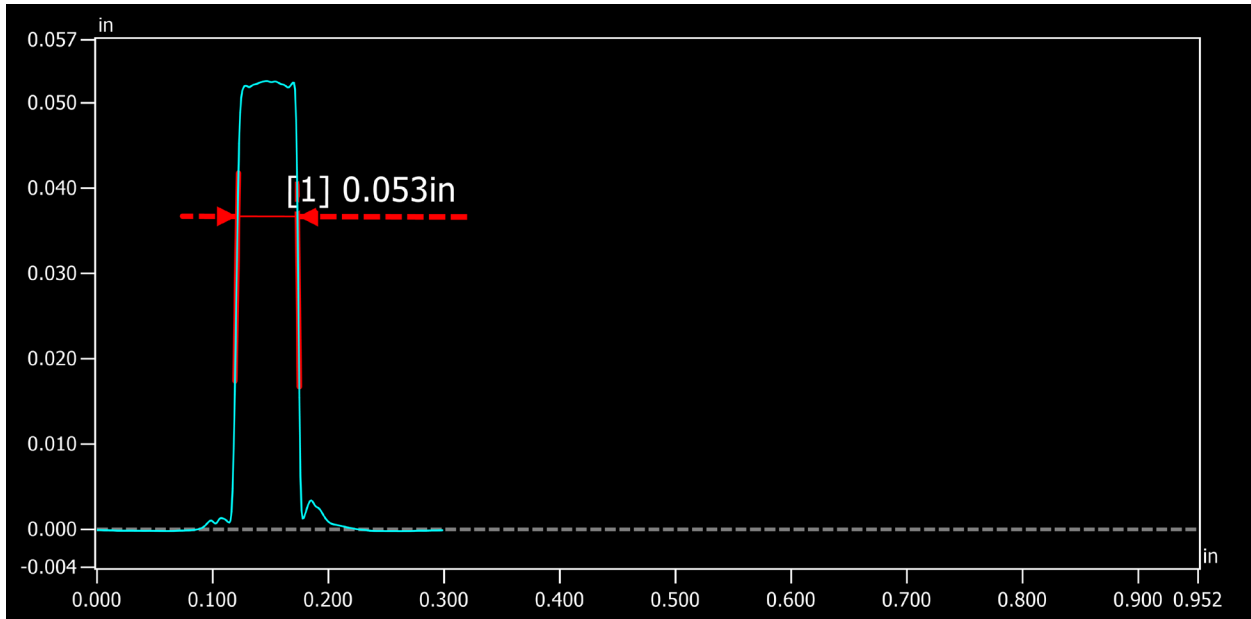
**Trip #3 (notionally  $k=0.052''$ ,  $b=0.052''$ )**



12x Optical image [Source: NASA].



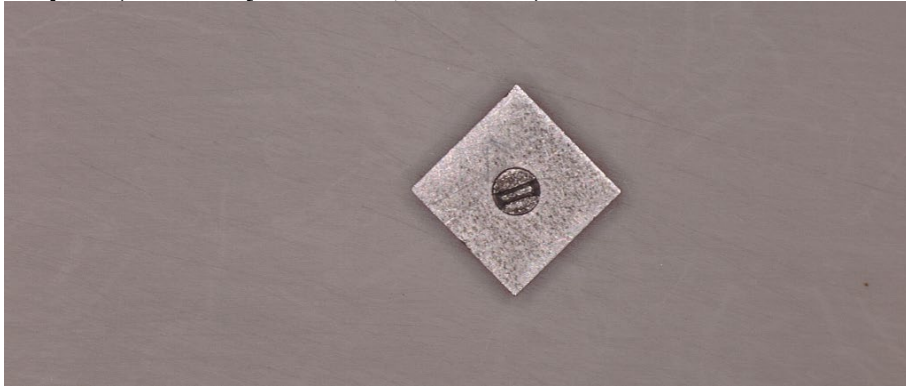
Profile locations shown (20 averages) [Source: NASA].



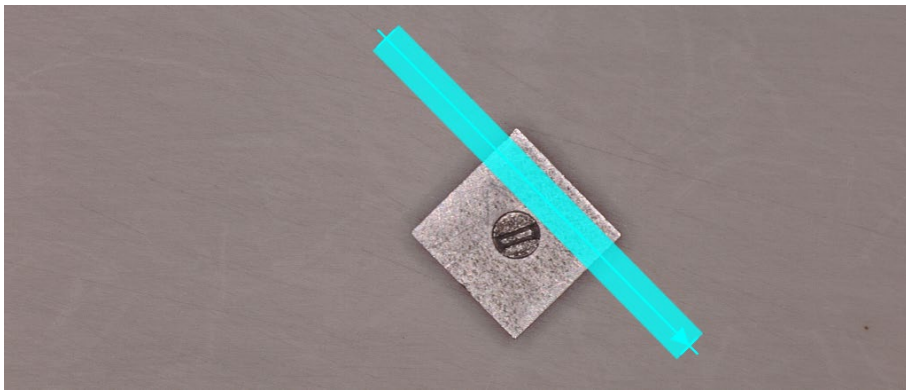
Measured  $k=0.052''$  and  $b=0.053''$

Appendix B - Digital Microscope Results

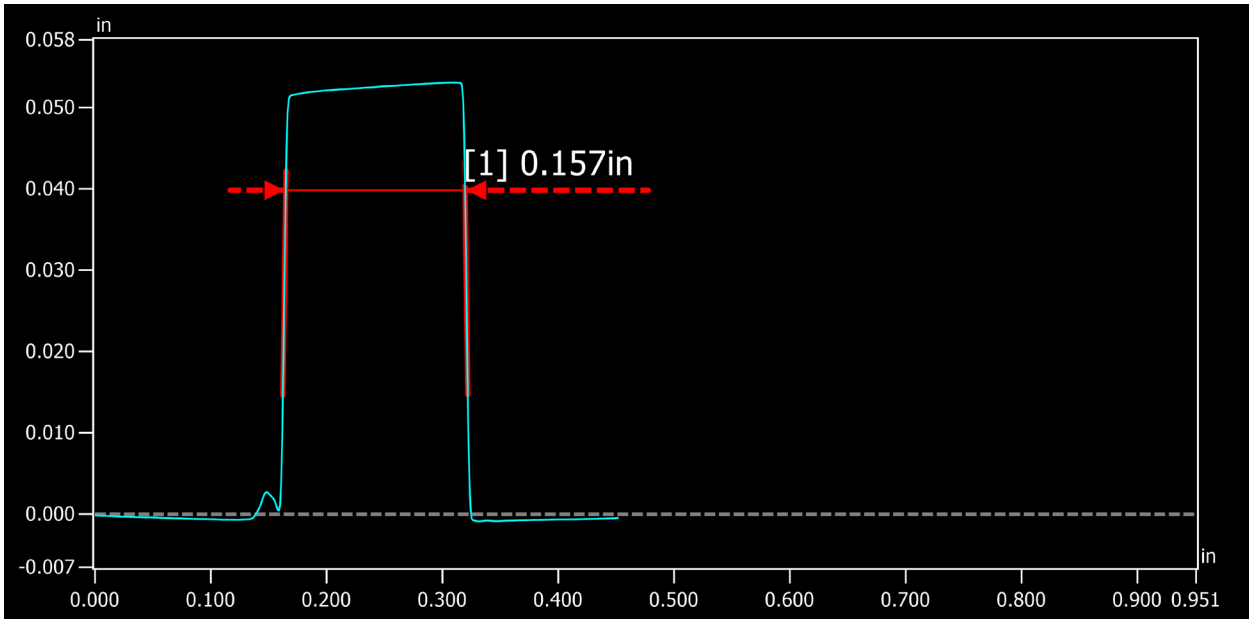
**Trip #4 (notionally  $k=0.052''$ ,  $b=0.156''$ )**



12x Optical image [Source: NASA].



Profile locations shown (20 averages) [Source: NASA].



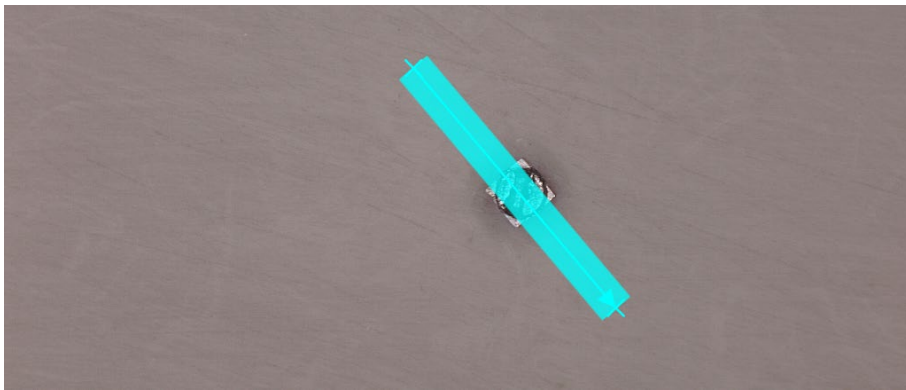
Measured  $k=0.052''$  and  $b=0.157''$

Appendix B - Digital Microscope Results

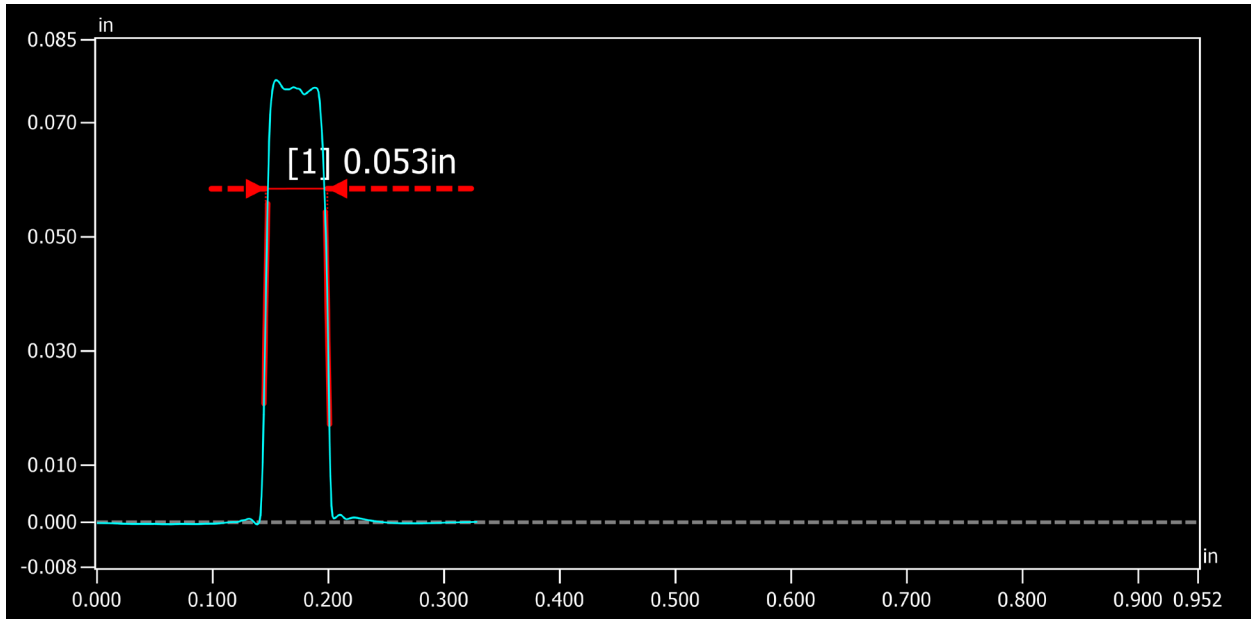
**Trip #5 (notionally  $k=0.076''$ ,  $b=0.052''$ )**



12x Optical image [Source: NASA].



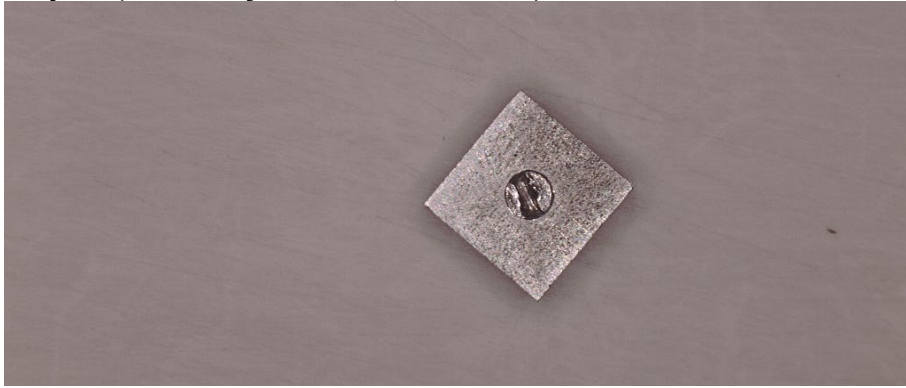
Profile locations shown (20 averages) [Source: NASA].



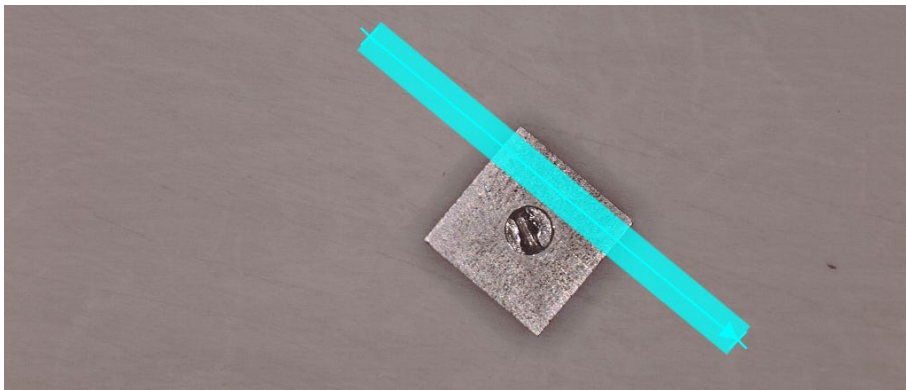
Measured  $k=0.077''$  and  $b=0.053''$

Appendix B - Digital Microscope Results

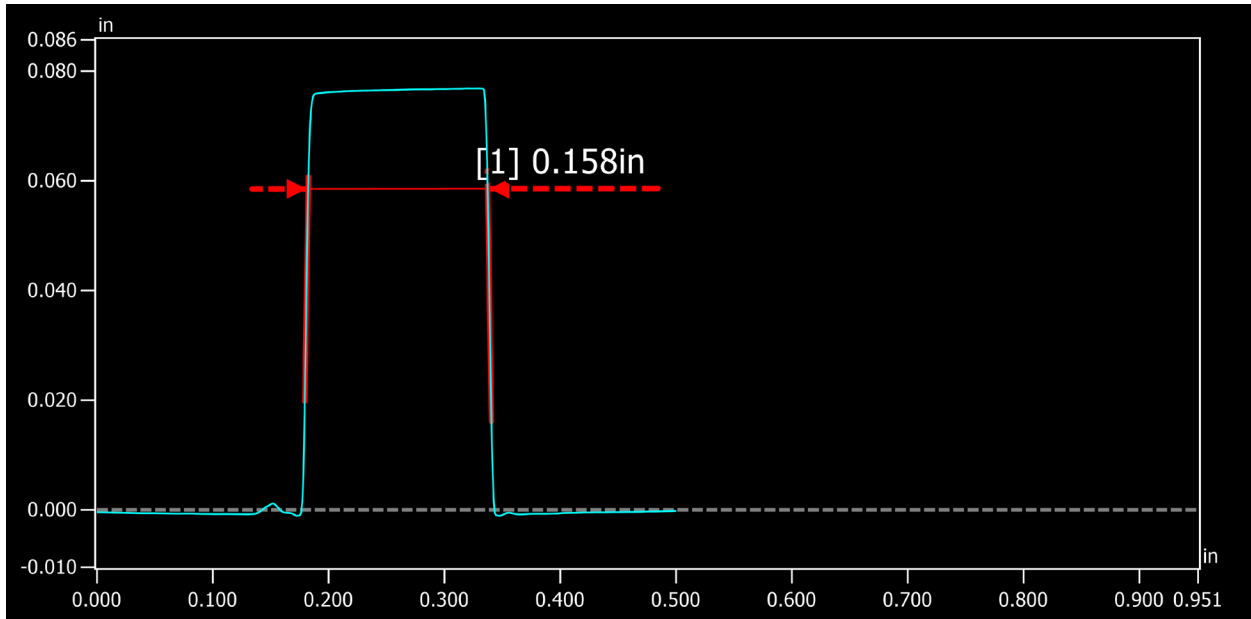
**Trip #6 (notionally  $k=0.076''$ ,  $b=0.156''$ )**



12x Optical image [Source: NASA].



Profile locations shown (20 averages) [Source: NASA].



Measured  $k=0.076''$  and  $b=0.158''$

Appendix B - Digital Microscope Results

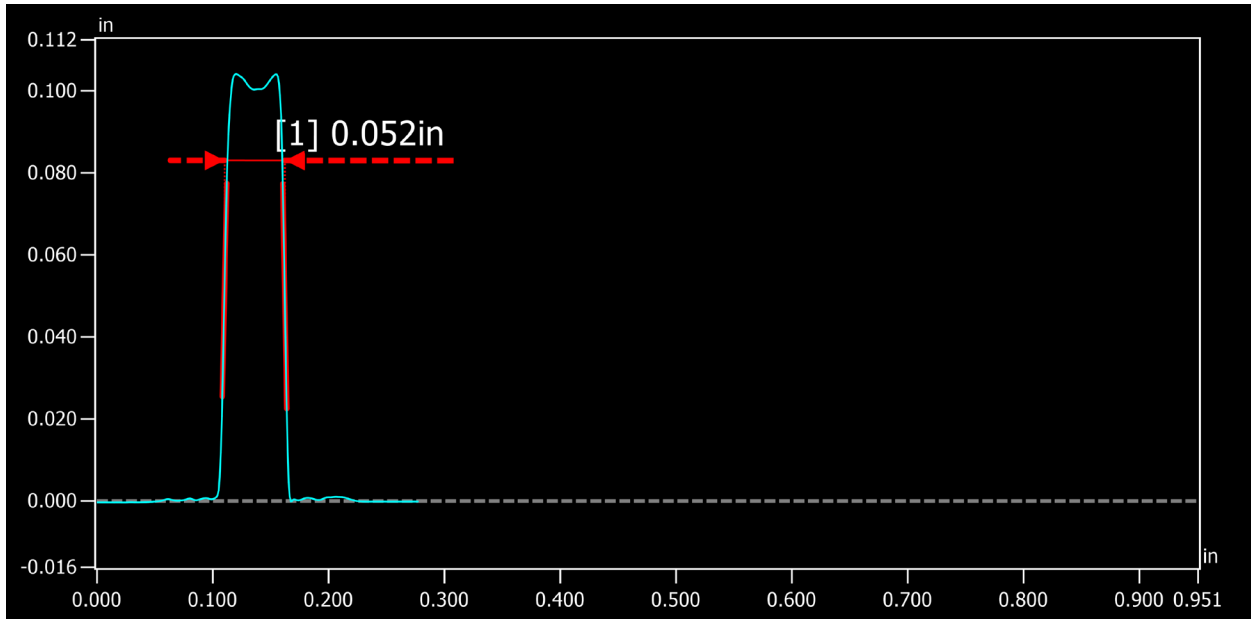
**Trip #7 (notionally  $k=0.100''$ ,  $b=0.052''$ )**



12x Optical image [Source: NASA].



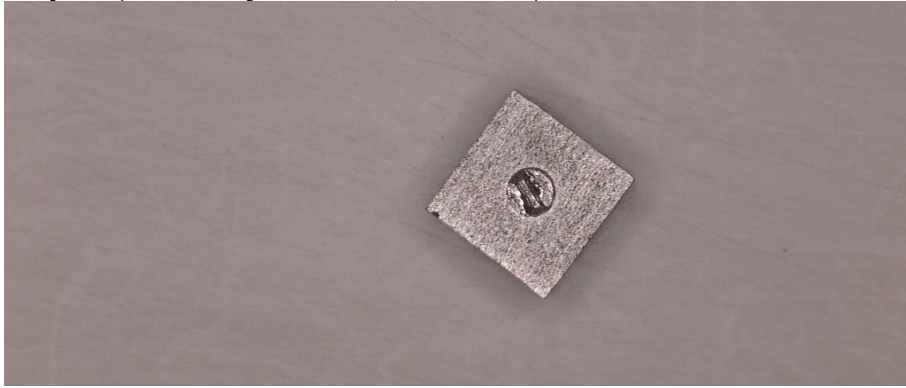
Profile locations shown (20 averages) [Source: NASA].



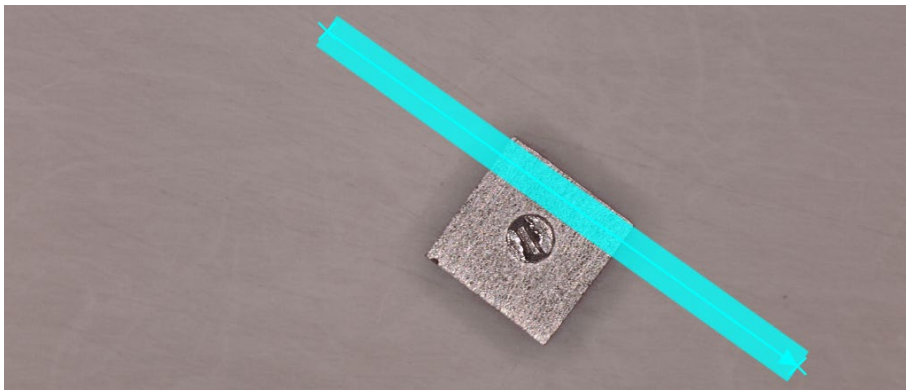
Measured  $k=0.102''$  and  $b=0.052''$

Appendix B - Digital Microscope Results

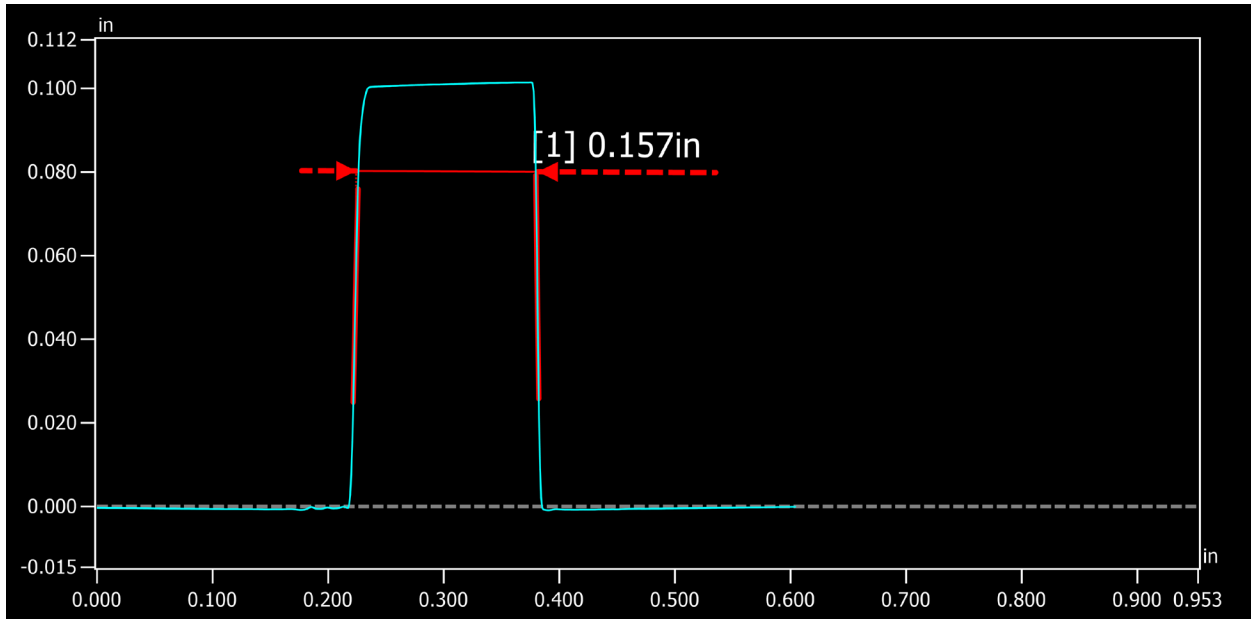
**Trip #8 (notionally  $k=0.100''$ ,  $b=0.156''$ )**



12x Optical image [Source: NASA].



Profile locations shown (20 averages) [Source: NASA].



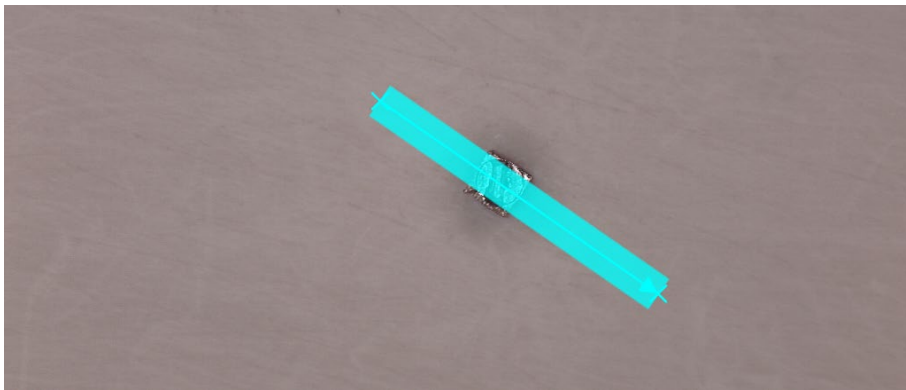
Measured  $k=0.100''$  and  $b=0.157''$

Appendix B - Digital Microscope Results

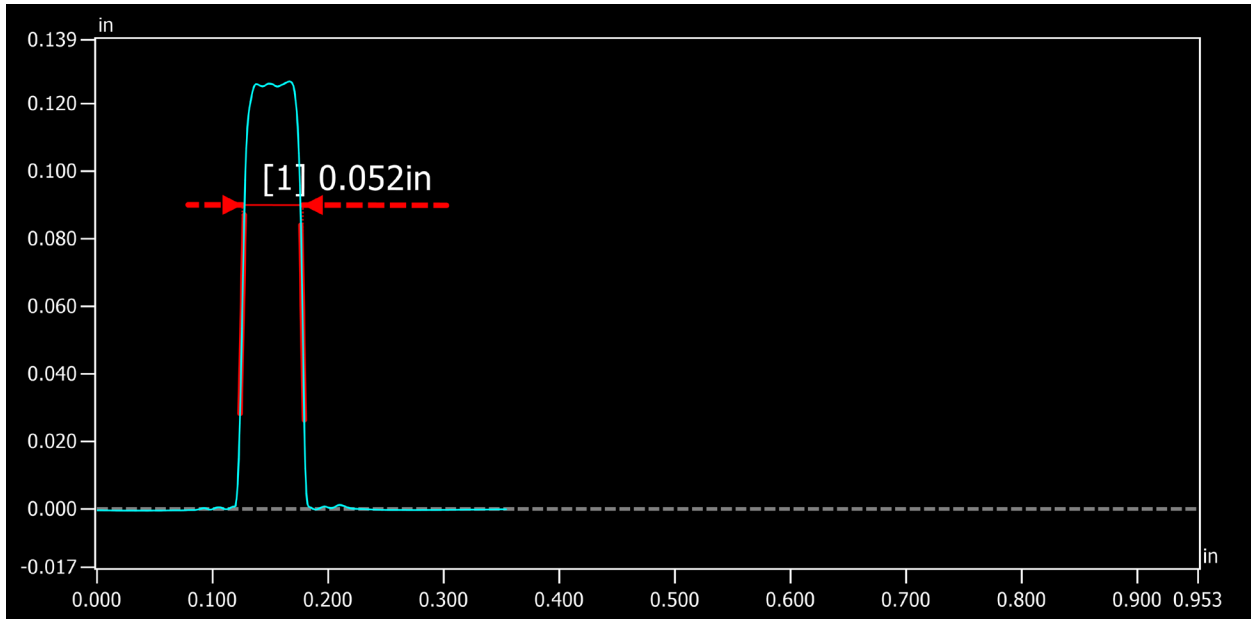
**Trip #9 (notionally  $k=0.124''$ ,  $b=0.052''$ )**



12x Optical image [Source: NASA].



Profile locations shown (20 averages) [Source: NASA].

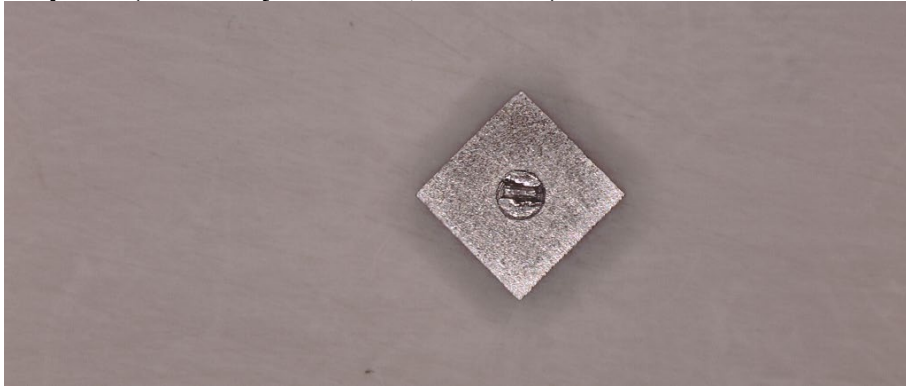


Measured  $k=0.124''$  and  $b=0.052''$

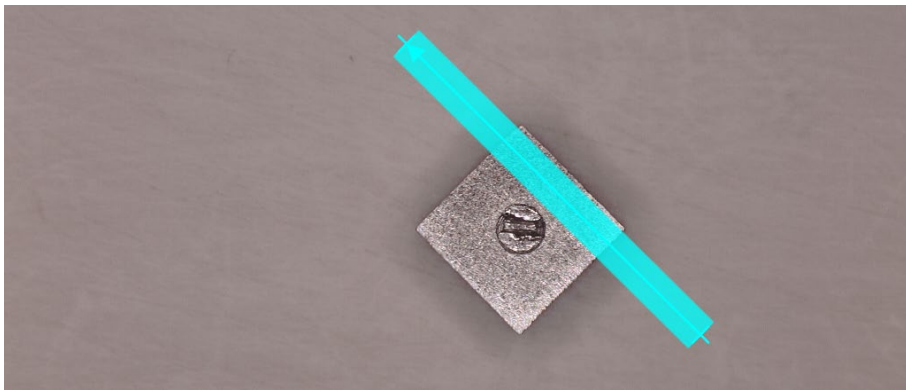


Appendix B - Digital Microscope Results

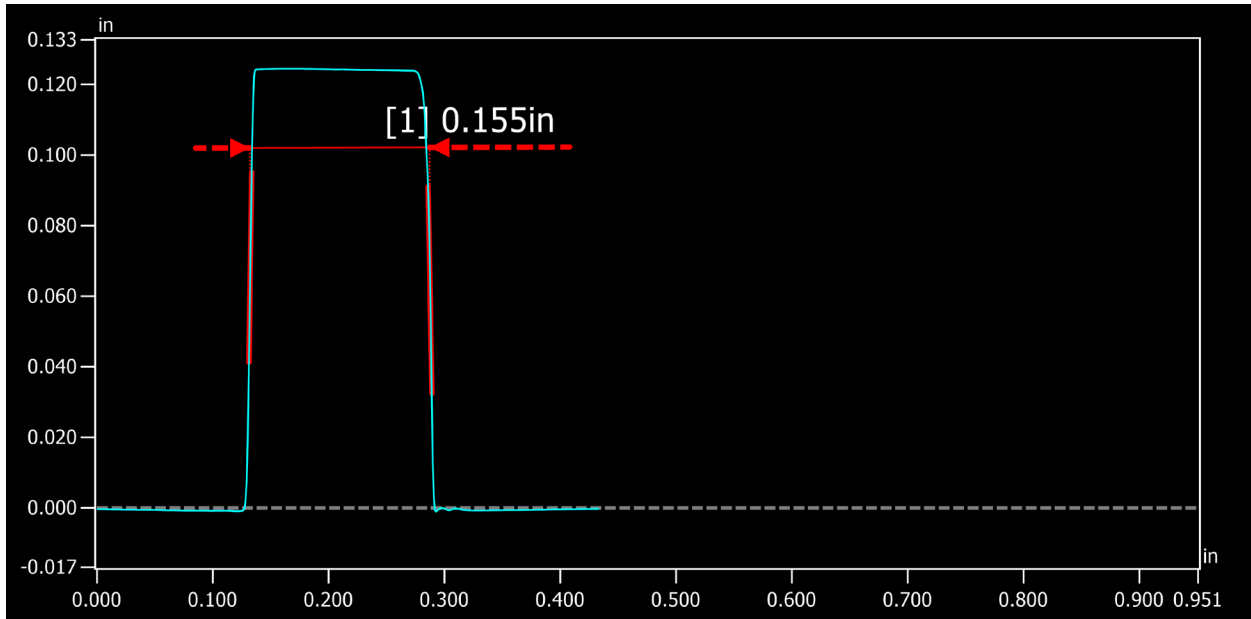
**Trip #10 (notionally  $k=0.124''$ ,  $b=0.156''$ )**



12x Optical image [Source: NASA].



Profile locations shown (20 averages) [Source: NASA].



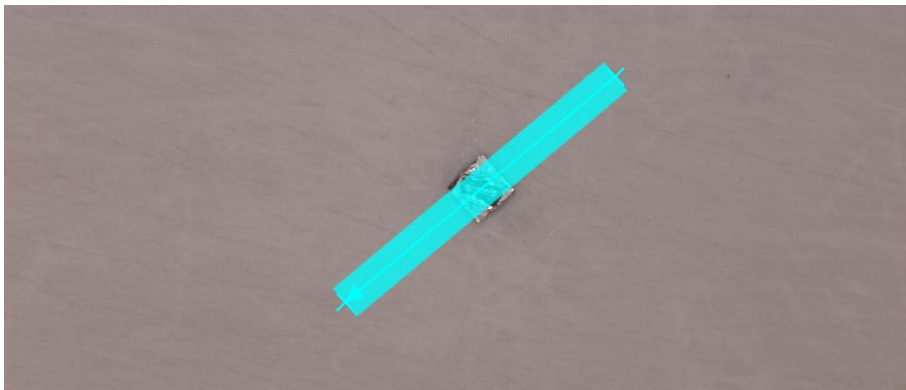
Measured  $k=0.124''$  and  $b=0.155''$

Appendix B - Digital Microscope Results

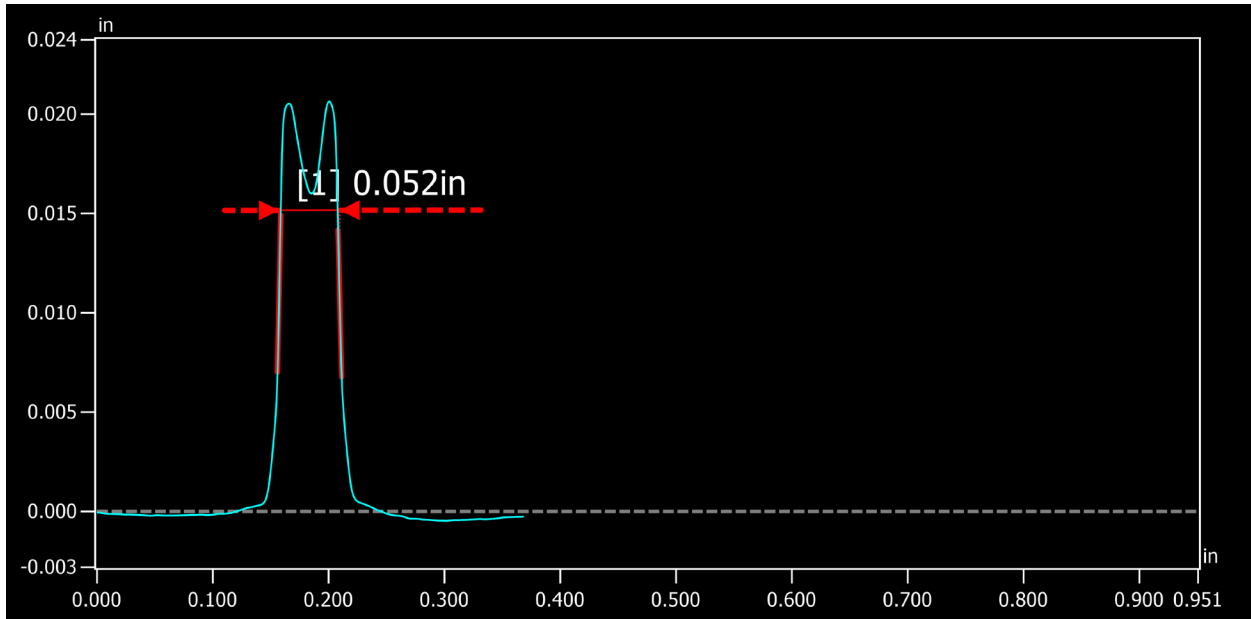
**Trip #11 (notionally  $k=0.018''$ ,  $b=0.052''$ )**



12x Optical image [Source: NASA].



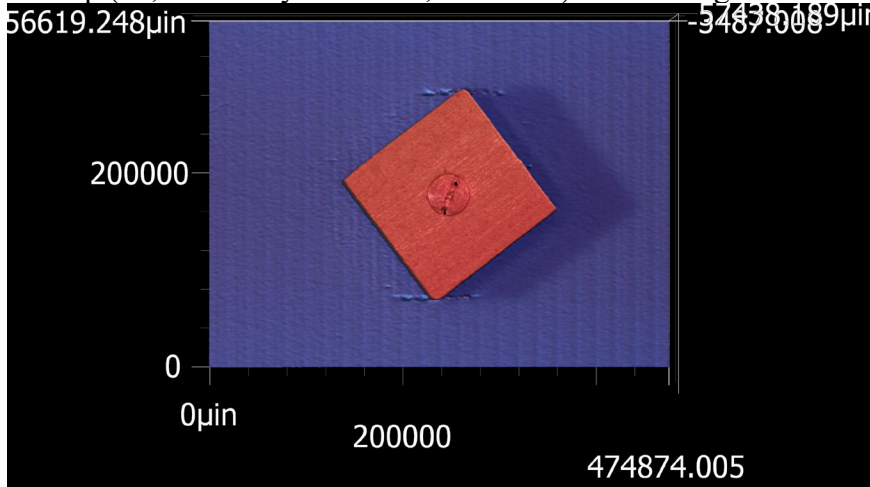
Profile locations shown (20 averages) [Source: NASA].



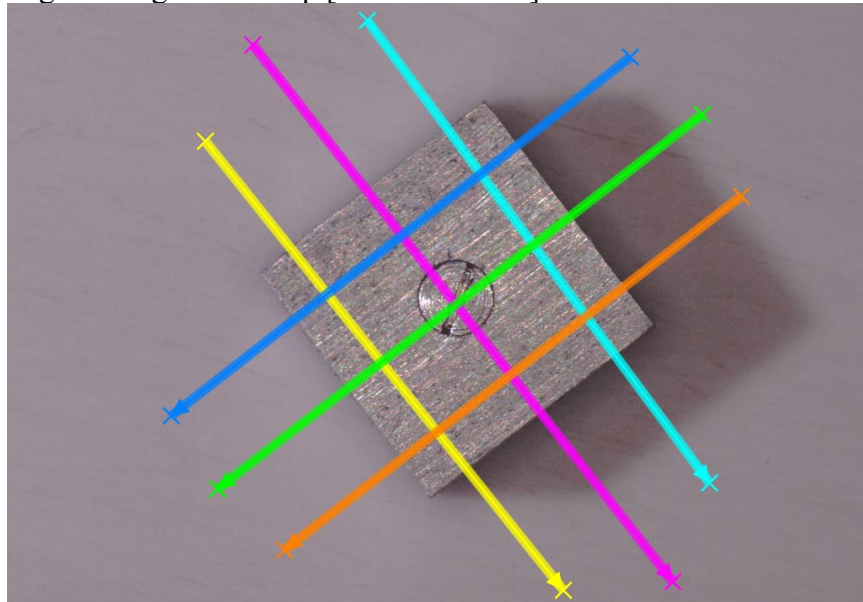
Measured  $k=0.021''$  and  $b=0.052''$

Appendix B - Digital Microscope Results

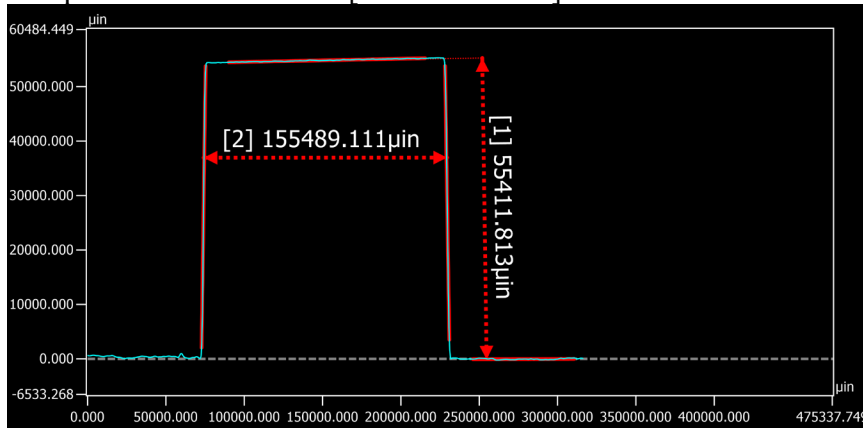
CL trip (#4, notionally  $k=0.052''$ ,  $b=0.156''$ ) used during Test 7067



Digital image of CL trip [Source: NASA].



Sample Line cut locations [Source: NASA].



Measured trip height  $k=0.055''$

Measured trip width  $b=0.155''$